

A research project report submitted by

Isobel Blower

as part of the requirement for the degree of:

MRes. Antimicrobials and Antimicrobial Resistance (AAMR)

This research project was carried out under the supervision of:

Dr. Michelle Buckner and Dr. Jeni Luckett

Supported by
wellcome trust

Date 30/07/2019

Word Count: 19328

Table of Contents

ABSTRACT **4**

ACKNOWLEDGEMENTS **5**

ABBREVIATIONS **6**

1. INTRODUCTION TO ANTIBIOTIC RESISTANCE **8**

1.1 DISCOVERY 8
1.2 RISE AND CAUSES OF ANTIMICROBIAL RESISTANCE (AMR) 9
1.3 TACKLING THE PROBLEM OF AMR 13

2. INVESTIGATING ANTIMICROBIAL RESISTANCE PLASMIDS **17**

2.1 ABSTRACT 17
2.2 INTRODUCTION 17
2.3 METHODS 21
2.3.1 Bacterial Strains used 21
2.3.2 Transfer of pNDM-HK gfp cat by electroporation 22
2.3.3 Transfer of pNDM-HK gfp cat by Filter Conjugation 23
2.3.4 Detection of pNDM-HK gfp cat by polymerase chain reaction (PCR) 23
2.3.5 Generation of K. pneumoniae Ecl8 mcherry nal^R and E. coli EC958c mcherry rif^R 24
2.3.6 Broth minimum inhibitory concentration (MIC) 25
2.3.7 Sequencing gyrA and rpoB 25
2.4 RESULTS 26
2.4.1 Transfer of pNDM-HK gfp cat into clinically relevant hosts by electroporation 26
2.4.2 Transfer of pNDM-HK gfp cat into clinically relevant E. coli strains by filter conjugation 27
2.4.3 Generation of mCherry E. coli and K. pneumoniae mutants and sequencing 28
2.5 DISCUSSION 30
2.5.1 Transfer of pNDM-HK gfp cat into E. coli and K. pneumoniae 30
2.5.2 Generation of E. coli mcherry and K. pneumoniae mcherry mutants 32

3 DEVELOPING TOOLS TO INVESTIGATE STAPHYLOCOCCUS AUREUS BIOFILM GROWTH **35**

3.1 ABSTRACT 35
3.2 INTRODUCTION 35
3.3 METHODS 40
3.3.1 Bacterial strains and growth media used 40
3.3.2 Growth media 41
3.3.3 Generation of phage lysate and phage transduction 42
3.3.4 MIC 42
3.3.5 Generation of allelic exchange vector 43
3.3.6 Growth curves 45

3.3.7 Biofilm models 45
3.3.8 Galleria mellonella infection models 46
3.4 RESULTS AND DISCUSSION 47
3.4.1 Phage transduction to create S. aureus JE2 lux 47
3.4.2 Knockout of 1984 in S. aureus SH1000 48
3.4.3 S. aureus growth in artificial saliva media 51
3.4.4 S. aureus biofilm bead models 53
3.4.5 Biofilms in artificial saliva media 54
3.4.6 S. aureus biofilms stained with fluorescent probes 57
3.4.7 In vivo virulence testing 60
3.4.8 Conclusions 62
4 FUTURE PERSPECTIVES 63
4.1 ANTIMICROBIAL RESISTANCE PLASMIDS 63
4.2 INVESTIGATION OF S. AUREUS BIOFILMS 65
REFERENCES 68

Abstract

The antibiotic resistance crisis is threatening the future of modern healthcare and the discovery of solutions will involve collaboration and investigation into multiple avenues of research. This work involved two projects, the first investigating plasmid transmission and the spread of antibiotic resistance genes (ARGs). The second focussed on developing tools to monitor *Staphylococcus aureus* biofilm growth.

ARGs can be spread between bacteria of the same or different species by horizontal gene transfer on plasmids. Transmission of plasmids can be specific to each host-plasmid interaction therefore it is important to monitor plasmid transmission in clinically relevant hosts. This project involved developing a fluorescence-based system used for monitoring the spread of ß-lactamase carrying plasmids. The system has been established for monitoring transmission of pCT and pKpQIL in single-species environments, the aim was to establish this with pNDM-HK, a globally disseminated AMR plasmid. The second focus was to develop the system with pCT and pKpQIL to enable monitoring of plasmid movement in multi-species environments. The assay can be used to screen for inhibitors of plasmid conjugation to prevent the spread of antibiotic resistance plasmids.

The second project involved developing tools for evaluation of *S. aureus* biofilm growth. Growth in biofilms protects bacteria from antibiotics and the host immune response making infections hard to clear. Phenotypic analysis of *S. aureus* biofilm growth was performed on ceramic beads as tooth models and cytodex beads which are used as supports in virulence models *in vivo*. Biofilms were visualised using confocal microscopy. Biofilms were grown in artificial saliva media to mimic biofilm growth in the mouth which is a reservoir for staphylococci that can disseminate around the body. A strain with a knockout of the *agr* system was analysed as this has a role in control of biofilm growth. Confocal microscopy was also used to determine the spatial heterogeneity of *S. aureus* biofilms to give insights for drug target development.

Acknowledgements

I would like to thank the Wellcome Trust, the University of Birmingham and the University of Nottingham for the opportunity to work on both of these projects. I would like to thank Dr Buckner and the members of the Piddock group in Birmingham for all their help and support during my first rotation project and with writing my report. I would also like to thank Dr Luckett, Dr Murray and members of the C69 lab in Nottingham for all their help and support with my lab work during my second project.

Abbreviations

Abbreviation	Meaning
agr	Accessory gene regulator
AIP	Autoinducing peptide
AMR	Antimicrobial resistance
aph	Aminoglycoside 3'-phosphotransferase
ARG	Antibiotic resistance gene
Bp	Base pairs
cat	Chloramphenicol acetyltransferase
CLSM	Confocal laser scanning microscopy
CTX-M	Cefotaximase modifying enzymes
erm	Erythromycin resistance gene
E. coli	*Escherichia coli*
EdU	5-ethynyl-2'-deoxyuridine
ESBL	Extended spectrum β-lactamase
gfp	Green fluorescent protein
GI	Gastrointestinal
HGT	Horizontal gene transfer
Inc	Incompatibility group
Kb	Kilobase
K. pneumoniae	*Klebsiella pneumoniae*
KPC	*Klebsiella pneumoniae* carbapenemases
LB	Lysogeny broth
LBA	Lysogeny broth agar
MCS	Multiple cloning site
MIC	Minimum inhibitory concentration

NDM	New Delhi metallo-ß-lactamase
nm	Nanometres
NTC	No template control
OD	Optical density
OPP	O-propargyl-puromycin
PBS	Phosphate buffered saline
PCR	Polymerase chain reaction
S. aureus	*Staphylococcus aureus*
TSA	Tryptic soy agar
TSB	Tryptic soy broth

1. Introduction to Antibiotic Resistance

1.1 Discovery

The discovery and use of antibiotics in the 20th century transformed medicine and saved millions of lives however the emergence and spread of antibiotic resistant bacteria is endangering the efficacy of these drugs (1). Antibiotics have been enormously successful in the treatment and prevention of infectious diseases and are the most successful drug category in the improvement of human health (2, 3). In addition to being used to treat a wide range of bacterial infections they are essential for prophylaxis, surgeries such as transplantation, chemotherapy and treating patients with chronic diseases. Antibiotics are essential for modern medicine and have extended life spans by changing the outcome of bacterial infections (1).

The modern era of antibiotics started with Paul Ehrlich and Alexander Fleming. Ehrlich had the idea that a 'magic bullet' drug could be used to target disease causing microbes without harming the host cells (4). He initiated a screening programme in 1904 using derivatives of a highly toxic drug, atoxyl, to find a drug which would combat syphilis. In 1909 he discovered a successful compound which was sold commercially as Salvarsan and which was the most prescribed drug until it was replaced by penicillin in the 1940s. Penicillin was discovered by Alexander Fleming in 1928 and was used widely in World War II for treatment of infectious diseases (3, 5). Penicillin was enormously successful however shortly after its discovery the spread of penicillin resistance became a substantial clinical problem so by the 1950s the advances of the previous decade were already threatened (1).

In response to the widespread use of penicillin and the emergence of resistance, more antibiotics were discovered leading to the 'golden age' for the discovery of antibiotic classes many of which are secondary metabolites from bacteria or fungi. Streptomycin was isolated from soil bacterium *Streptomyces*

griseus in 1944 which initiated a worldwide search for antibacterial natural products (4, 6). The main antibiotic classes are displayed in Table 1.

Table 1. Main antibiotic classes (7)

Class	Mechanism of action	Example(s)
ß-lactams	Inhibit cell wall biosynthesis	Penicillin, cephalosporins
Sulfonamides	Inhibit folic acid synthesis, prevent growth and multiplication of bacteria	Prontosil
Aminoglycosides	Inhibit protein synthesis	Streptomycin, gentamycin
Tetracyclines	Inhibit protein synthesis	Tetracycline, doxycycline
Chloramphenicol	Inhibit protein synthesis	Chloramphenicol
Macrolides	Inhibit protein synthesis	Erythromycin, azithromycin
Glycopeptides	Inhibit cell wall biosynthesis	Vancomycin
Ansamycins	Inhibit RNA synthesis	Rifamycin
Quinolones	Interfere with DNA replication and transcription	Ciprofloxacin, nalidixic acid
Streptogramins	Inhibit protein synthesis	Pristinamycin IA
Oxazolidonones	Inhibit protein synthesis	Linezolid, cycloserine
Lipopeptides	Disrupt cell membrane functions	Daptomycin

The success of antibiotics and discovery of novel antibiotic classes was such that, in 1962, Nobel laureate Sir Frank Macfarlane Burnett wrote “One can think of the middle of the 20th century as the end of one of the most important social revolutions in history, the virtual elimination of the infectious diseases as a significant factor in social life” (8). From the late 1960s to the early 1980s the pharmaceutical industry introduced many new antibiotics however the pipeline then began to dry up so that fewer new classes were introduced (1, 8). Almost all antibiotics in clinical use belong to classes discovered during this period. The production of antimicrobials is unable to keep up with the increase in antibiotic resistant infections and these have become a threat meaning infectious diseases remain one of the major causes of human morbidity and mortality (2).

1.2 Rise and causes of antimicrobial resistance (AMR)

The antibiotic resistance crisis has been attributed to the overuse and misuse of these medications along with lack of antibiotic discovery by the pharmaceutical industry (1). The pipeline of antibiotic discovery has waned and is currently insufficient to deal with the threat of resistant bacteria (5, 8). As

early as 1945 Alexander Fleming predicted that the overuse of antibiotics would drive the emergence of resistance, and currently the benefits of antibiotics are being lost due to the rise of drug resistant strains (1). Resistance has been reported against nearly all antibiotics in clinical use (3). A timeline of the development of antibiotic resistant infections is shown in Figure 1.

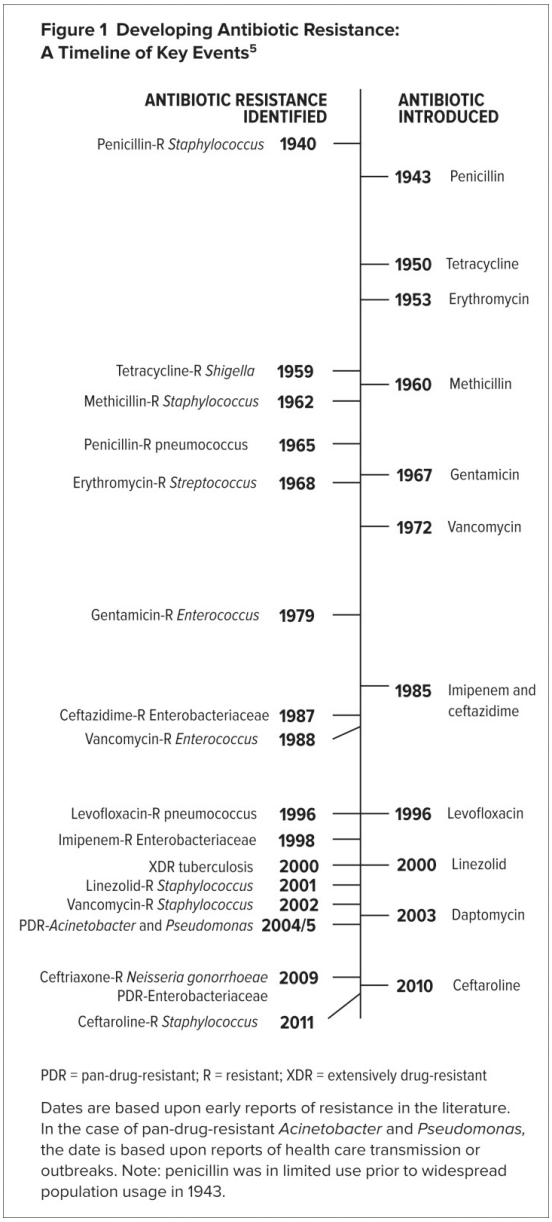


Figure 1. Timeline of the emergence of resistant strains of bacteria compared to when the antibiotic was introduced (1)

AMR arises due to bacterial adaption to antimicrobial attack enabled by their genetic plasticity (9). The selective pressure of the antibiotic will remove

sensitive bacteria leaving resistant bacteria as a result of natural selection (10). Resistance can be intrinsic where the bacteria is resistant without genetic alteration such as mycoplasma resistance to beta-lactams as they lack peptidoglycan in the cell wall (7). However antibiotic resistance is largely due to acquired resistance in a bacterial population that was originally susceptible to a compound. This is usually caused by mutations in genes often associated with the drug's mechanism of action or through acquisition of foreign resistance genes by horizontal gene transfer (HGT) (2, 9, 11). Resistance can be through decreased drug uptake, increased export of the drug, inactivation of drug targets, introduction of a new drug resistant target (acquisition of *mecA* conferring methicillin resistance), hydrolysis of the antibiotic (beta-lactamases) or modification of the antibiotic (aminoglycoside modifying enzymes) (7, 9).

Resistance can be gained by acquisition of extracellular DNA carrying antibiotic resistance genes by transformation, transduction or conjugation (9). There are many DNA elements which have been found to transfer antibiotic resistance genes including self-replicating plasmids, prophages, transposons and integrons. This enables the spread of antibiotic resistance between bacteria of different species (10). Plasmids can carry resistance to multiple antibiotics therefore selecting for resistance to one antibiotic may result in selection for resistance to others simultaneously if the genes are carried on the same plasmid (7). Spread of AMR plasmids has led to the global spread of antibiotic resistance genes and the emergence of pan resistant strains. For example, CTX-M, a plasmid encoded extended spectrum ß-lactamase (ESBL) found in *Enterobacteriaceae* is the most prevalent ESBL and is spread globally causing ß-lactam resistance in *E. coli* and *K. pneumoniae* (9).

Resistance to antibiotics can also be physiological where it is only seen during certain growth conditions such as in bacterial biofilms. Bacteria such as *Pseudomonas aeruginosa* and *Staphylococcus aureus* adopt a sessile biofilm lifestyle which are notoriously difficult to eradicate with antibiotic treatment (7). Cells in the biofilm display altered gene expression and lower growth rates due to anoxic conditions and low nutrient levels. These slow growing cells are

tolerant to high concentrations of antibiotic. The biofilm matrix also acts as a diffusion barrier to antibiotics preventing them from penetrating to cells in the centre of the biofilm. After antibiotic treatment persistor cells are left which are not eradicated by the antibiotic treatment, these can activate and re-establish infection (12-14).

There are many human factors which are deemed responsible for the rise and spread of AMR including the overuse and misuse of antibiotics. There is a direct correlation between antibiotic consumption and the dissemination of antibiotic resistant strains as overuse of antibiotics increases the selective pressure for generation of resistance (11). Studies have shown that the antibiotic treatment chosen or the duration of treatment is wrong in 30-50% cases (1). This is often due to the deficiency in rapid and accurate diagnosis of a causative pathogen and the susceptibility of this pathogen to particular antibiotics (11). Incorrectly prescribed antibiotics contribute to the promotion of resistant bacteria as subinhibitory concentrations of antibiotic can promote antibiotic resistance development (1).

Overuse and misuse of antibiotics is promoted by the unregulated sale of these drugs in many countries. Antibiotics are cheap and easily accessible and can even be purchased online. Hoarding of these and incorrect application will lead to an increase in the generation of resistance (5, 11). Antibiotic use in agriculture is another driver for the emergence and spread of antibiotic resistance. Antibiotics are widely used as growth supplements or prophylactically in livestock, 80% antibiotics sold in the US are used in animals (2015) (1, 8, 11). Resistant bacteria and antibiotics can then pass to humans when they consume meat. Additionally, up to 90% antibiotics given to livestock are excreted in stool or urine and are distributed further through fertilisation. Increasingly abundant and diverse AMR genes are seen in agricultural settings (1, 11).

The development of new antibiotics cannot keep up with the emergence of resistance. This problem is compounded by the fact that many pharmaceutical

companies are leaving the field of antibiotic research due to the lack of financial incentive. Antibiotic development is not economically beneficial as the drugs are used for short periods of time, are low cost and novel antibiotics will be held back for last resort use. Treatments for chronic infections are much more profitable and so there is no incentive for pharmaceutical companies to develop novel antimicrobials (1).

1.3 Tackling the problem of AMR

AMR is a substantial global health and economic burden and there is an urgent need for solutions in order to avoid entering a post antibiotic era. Coordinated efforts will be required to implement policies and invigorate research to help manage the crisis (1). If antibiotics continue to be used in the same way resistance will continue to emerge (8). The global spread of AMR is endemic, and the emergence of pan resistant bacteria has affected practice in every field of medicine. Bacteria are becoming resistant to nearly all drug options creating situations reminiscent of the pre-antibiotic era (1).

In 2016 the UK government commissioned a review on AMR which was performed by economist Jim O'Neill. The purpose of this was to analyse the problem of antibiotic resistant bacteria and propose recommendations to tackle the issue. This report predicted that by 2050 10 million lives per year will be at risk from AMR and the loss in economic output between now and 2050 is likely to be 100 trillion US dollars unless strategies are put in place to slow the impact of drug resistant infections. However, O'Neill states that the AMR crisis is not insurmountable. He outlines 4 main interventions which involve a combination of policy intervention and research. These are increasing global public awareness, tackling the supply problem, reducing antibiotic usage in humans and animals and reducing antibiotic use in agriculture (15).

Policies which improve global awareness of AMR through education will reduce the public demand for antibiotics when use is unnecessary. Antibiotic stewardship must be modernised to involve the general public and make them aware of the issue (8). Surveillance of drug resistance and antibiotic

consumption should be performed in order to collate data globally (8, 15). Additionally, new, rapid diagnostics must be developed. This will reduce the unnecessary use of antibiotics and can lead to targeted therapies. (8, 15). For example, rapid strep tests reduce the antibiotic prescriptions for control of pharyngitis (8).

Efforts must be made to prevent infection in the first place. This can be done by improving hygiene and sanitation, particularly in developing countries as living in communities in close proximity in areas with poor sanitation provides the opportunity for proliferation of infectious disease (11). Reducing the number of people infected will reduce the demand for antibiotic treatment, therefore reducing the emergence of resistant strains. This can be achieved by improving water supply and sewage treatment in developing countries. In developed countries the spread of infections in hospitals must be prevented through hand washing and isolation or cohorting of infected patients (8, 15, 16).

The use of antibiotics in agriculture as growth promoters must be restricted as it is an unnecessary use of antibiotics. In Denmark the use of antibiotic growth promoters was banned and an improvement was seen in swine productivity showing that use of antibiotic growth promoters is not essential in agriculture (17). In particular last resort antibiotics must not be used in agriculture, the efficacy of these drugs must be preserved for use in clinical infections (16).

As well as introduction of policies to reduce the spread and development of AMR there is an urgent need for new antimicrobials. 90% antibiotics used in clinics are derived from microorganisms. Many of these were discovered during the golden age of antibiotic discovery (18). Discovery of natural product antibiotics has waned but there are still many ecological niches which could be investigated with novel screening techniques to identify new compounds (5, 18). In 2008 more than 1000 novel natural product compounds were isolated from marine microorganisms and there is a vast reservoir of these which have not been explored. Investigation of these and more natural products will

require the collaboration of pharmaceutical companies, academia and biotechnology companies to screen the large number of compounds required to end up with an antibiotic that will make it to the clinic (16, 18). Currently pharmaceutical companies are leaving the field of antibiotic discovery so there needs to be incentives for them to invest. This could include market entry awards such as the payment of $1 billion per drug for effective treatments coming to the market (15).

Current antimicrobials can be improved through modification producing compounds which are less sensitive to resistance mechanisms and are less toxic to the patient however resistance will ultimately rise against these compounds (5). Therefore alternative therapies are needed such as immunisation through vaccines, phage therapy, probiotics or immunostimulants (5, 16). Investigation of novel approaches for prevention and treatment of infectious diseases must be encouraged (16). As well as focussing on compounds which kill bacteria, compounds which reduce bacterial virulence can be developed. These will mean bacteria cannot cause infection but will reduce the pressure on the bacteria to acquire mutations and can be used in combination with classic antibiotics (5, 18) For example, inhibiting endotoxin synthesis will mean the bacteria will not be killed but will not cause disease, starving bacteria of nutrients such as iron will mean they cannot proliferate in the host (8). Inhibition of the spread of antibiotic resistance genes could help to prevent the spread of antibiotic resistance, this could be done through inhibiting plasmid conjugation (19, 20). Antibiotic resistance genes are often disseminated on plasmids so inhibition of the spread of these will reduce AMR spread and these can be used in combination with classic antibiotics (21).

AMR is an increasingly serious threat to global health and requires solutions from government, researchers and members of the public. The aim of this work is to discuss two projects which both aim to address issues relating to the AMR crisis. The first project focussed on monitoring the transmission of AMR plasmids involved in spread of antibiotic resistance genes worldwide. The

second project focussed on developing tools for investigation of *Staphylococcus aureus* biofilms which are challenging to treat and cause persistent and chronic infections increasing morbidity and mortality.

2. Investigating Antimicrobial Resistance Plasmids

2.1 Abstract

Horizontal gene transfer of antibiotic resistance plasmids plays a major role in the spread of antibiotic resistance genes (ARGs) particularly extended spectrum β-lactamases (ESBLs). Monitoring transmission of these plasmids informs about how ARGs spread. The Buckner group has established a fluorescence-based system to measure transmission of clinically relevant ESBL carrying plasmids expressing *gfp* into cells expressing *mcherry* chromosomally. This is set up with pCT bla_{CTX-M} *gfp* and pKpQIL bla_{KPC} *gfp* in *Escherichia coli* and *Klebsiella pneumoniae.* Flow cytometry is used to detect transmission events and this assay is usedmto identify conjugation inhibitors. One aim of this project was to develop this system with pNDM-HK *gfp.* In order to do this the plasmid must be transferred to clinically relevant strains to use as plasmid donors. This was attempted through electroporation and conjugation assays however the plasmid was not able to be moved into clinically relevant strains therefore further work would be required to complete this. The other aim of this project involved developing the system to use *mcherry* expressing bacteria as *gfp* expressing plasmid donors. A model such as this would enable prediction of how plasmids would spread in complex multispecies environments. The first step of this was to create unique antibiotic resistance mutations in *E. coli* and *K. pneumoniae* expressing *mcherry* to enable selection of transconjugants when mated with pCT bla_{CTX-M} *gfp* and pKpQIL bla_{KPC} *gfp.* These will be used as donors in plasmid transmission assays.

2.2 Introduction

Antimicrobial resistance (AMR) is one of the largest threats to healthcare in the 21st century and treatment of infections caused by antibiotic resistant bacteria is becoming increasingly challenging (15, 22). The production of novel antibiotic

drugs is unable to keep up with the increase in emergence of resistant infections therefore novel approaches to control AMR are needed such as preventing the spread of antibiotic resistance genes (ARGs) (19, 22, 23).

ARGs are often transferred between Gram-negative bacteria by horizontal gene transfer (HGT) particularly via plasmid conjugation (14, 24, 25). This involves spread of plasmids from one bacterial cell to another via direct contact of donor and recipient cells through a conjugational pilus (26). Plasmids are usually circular, self-replicating pieces of DNA which can encode genes for a variety of functions including antibiotic resistance (24, 27). They are characterised based on incompatibility groups (Inc) which are defined by the inability of related plasmids to be maintained in the same cell as they use the same replication or partitioning mechanisms (28).

Plasmid conjugation plays a major role in the spread of ARGs due to the ability of plasmids to acquire genes from mobile genetic elements and replicate in multiple host species (29, 30). The emergence of multidrug resistant bacteria is frequently linked to the spread of conjugative plasmids (30). ARGs transferred on plasmids can pose a serious threat to healthcare, examples of these include extended spectrum ß-lactamases (ESBLs) such as cefotaximase modifying enzymes (CTX-M), New Delhi metallo-ß-lactamase (NDM) and *Klebsiella pneumoniae* carbapenemases (KPC). These can be carried on multiple, highly variable plasmids which often carry resistance to other classes of antibiotics, further complicating treatment (27, 31).

Previously it has been hypothesised that due to the fitness costs plasmids confer on their hosts, once the selective pressure which selects for their presence is removed, the plasmid will not be sustained in the population (32). This would mean AMR genes should be lost in the absence of antibiotic selection for example during antibiotic cycling however recent studies have shown that plasmids carrying AMR genes can be sustained even in the absence of antibiotic pressure (33, 34).

Inhibition of conjugation and plasmid persistence would be effective in reducing ARG dissemination and removing a plasmid from a population (19, 21, 27, 33). Inhibiting conjugation would reduce transfer of ARGs and lead to removal of plasmid reservoirs of ARGs providing an alternative method of tackling antibiotic resistance (23). Plasmid persistence and transfer can be specific to each plasmid host combination therefore it is important to investigate the interaction with different plasmids in multiple clinically relevant hosts (35). Three significant AMR plasmids were investigated in this study; pNDM-HK-*bla*$_{\text{NDM-1}}$, pCT-*bla*$_{\text{CTX-M}}$ and pKpQIL-*bla*$_{\text{KPC}}$. These are all widely disseminated in Enterobacteriaceae species and their spread attributed to HGT (36, 37) (38-41).

pNDM-HK carries *bla*$_{\text{NDM-1}}$, this can hydrolyse a wide range of carbapenem antibiotics rendering them ineffective (42). Plasmids carrying *bla*$_{\text{NDM-1}}$ have been shown to be highly capable of transfer and rearrangement meaning the potential for HGT and acquisition of ARGs is high (37, 42). pNDM-HK is an IncL/M plasmid, these usually have low copy number and can survive in a number of hosts (29). pCT is an IncK plasmid often associated with carriage of ESBLs including *bla*$_{\text{CTX-M}}$ genes which are a major worldwide problem (43-45). Horizontal transfer of *bla*$_{\text{CTX-M}}$ genes on plasmids such as pCT is fundamental to their global spread (36). pCT is highly stable in the absence of antibiotic pressure and is associated with highly pathogenic *E. coli* strains including the globally disseminated ST131 clonal group (34, 36). pKpQIL is a self-conjugative IncFII-like plasmid originally from *K. pneumoniae* and was first defined from *K. pneumoniae* ST258 isolate in 2006 (41). Horizontal spread of pKpQIL plasmids has been shown to be responsible for the dissemination of KPC carbapenemases (38-41).

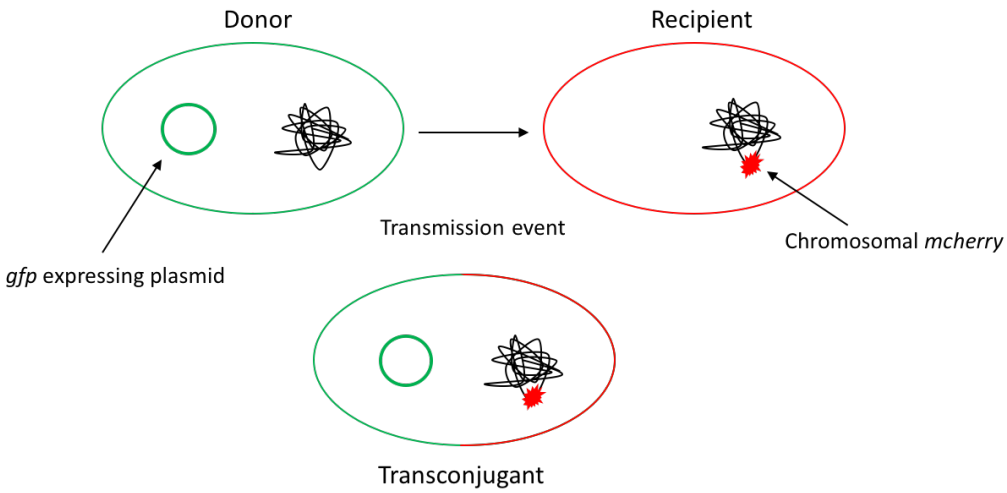


Figure 2. Outline of the assay used to detect plasmid transmission

Investigating how AMR plasmids move between bacteria is important in monitoring how ARGs are likely to spread and determining ways of inhibiting this (30). The Buckner group have developed a flow-cytometry based assay for monitoring plasmid transmission. *mcherry* is inserted into the chromosome of recipient cells and green fluorescent protein (*gfp*) into the plasmid (Figure 2). Donors fluoresce green, recipients fluoresce red and after plasmid transmission transconjugants fluoresce green and red. Flow cytometry is used to quantify the proportion of cells the plasmid has transferred into. This system is established to monitor pCT *gfp* and pKpQIL *gfp* transmission in clinically relevant *E. coli* and *K. pneumoniae* strains and is used to screen for potential inhibitors of conjugation. Part of the focus of this project was to develop this assay with pNDM-HK *gfp* by moving pNDM-HK *gfp cat* into clinically relevant *E. coli* and *K. pneumoniae* strains to be used as plasmid donors. The pNDM-HK *gfp cat* construct used had *gfp* and *cat* (chloramphenicol acetyltransferase) conferring chloramphenicol resistance for selection in the place of $bla_{\text{NDM-1}}$.

The other focus of this project was to develop a modified assay with pCT *gfp* and pKpQIL *gfp* to enable monitoring of plasmid transmission in multi-species environments. This is not possible in the current system as all plasmid recipients must be tagged with *mcherry* for detection. In the modified system plasmid donors will encode *mcherry* chromosomally so donors will fluoresce

green and red and transconjugants will fluoresce green, recipient cells do not need modification. In order to determine the cell types the plasmid has transferred to, fluorescence activated cell sorting and confocal microscopy can be used. To begin developing this system, this project aimed to select *E. coli mcherry* and *K. pneumoniae mcherry* with resistance to unique antibiotics. This would allow selection of transconjugants to use as plasmid donors after the bacteria were mated with pCT *gfp* or pKpQIL *gfp.* This will enable screening for inhibitors of plasmid transfer in multispecies environments such as the GI tract.

Discovery of novel ways of tackling the problem of antibiotic resistance is important and through monitoring plasmid conjugation and identifying inhibitors it will be possible to reduce the spread of AMR plasmids which will reduce the dissemination of ARGs.

2.3 Methods

2.3.1 Bacterial Strains used

Bacterial strains used are displayed in Table 2. Bacteria were cultured in lysogeny broth (LB) (Sigma-Aldrich) with antibiotics added as required. *E. coli* SW105 was grown at 30^{o}C whereas other strains were grown at 37^{o}C. Overnight cultures were grown with aeration by shaking at 200 rpm. Bacterial stocks were prepared on Protect beads (Thermofisher) and stored at -20 ^{o}C for short term or -80 ^{o}C for long term storage. Antibiotics were sourced from Sigma-Aldrich and stock solutions were created at 100 mg/mL. All strains used had been cured of any plasmids.

Table 2. Bacterial strains used in this study

Strain	Description	Antibiotic resistance	Use
SW105	*E. coli* carrying pNDM-HK-*gfp-cat*	Chloramphenicol (50 µg/mL)	pNDM-HK-*gfp-cat* donor
DH10B	*E. coli* cloning strain with high transformation efficiency	N/A	pNDM-HK recipient (electroporation)
ST131 EC958c	*E. coli* ST131 cured of pEC958	Nalidixic acid (128 µg/mL)	
Ecl8 rif^R	*K. pneumoniae* Ecl8 with *rpoB* mutation	Rifampicin (100 µg/mL)	
ST131 EC958c rif^R	*E. coli* ST131 cured of pEC958 with *rpoB* mutation	Rifampicin (100 µg/mL), Nalidixic acid (128 µg/mL)	pNDM-HK recipient (filter conjugation)
ST131 B104 rif^R	*E. coli* B104 with *rpoB* mutation	Rifampicin (100 µg/mL)	
ST131 EC958c *mcherry*	*E. coli* EC958c with *mcherry aph* inserted into *putPA* intergenic region	Kanamycin (50 µg/mL)	Mutant selection
Ecl8 *mcherry*	*K. pneumoniae* Ecl8 with *mcherry aph* inserted into *putPA* intergenic region	Kanamycin (50 µg/mL)	

2.3.2 Transfer of pNDM-HK *gfp cat* by electroporation

Overnight cultures of recipient bacteria were diluted in LB and re-grown to OD_{600} 0.7 nm. The culture was cooled on ice, centrifuged and washed twice with 50 mL ice cold 15% glycerol (Fisher Scientific) before final suspension in 500 µL 15% glycerol. pNDM-HK-*gfp-cat* was extracted from *E. coli* SW105 using Qiagen QIAprep spin miniprep kit with a final elution in 30 µL water. pNDM-HK *gfp cat* was added to 50 µL electrocompetent cells, 5 µL to one aliquot and 15 µL to another. A positive control with 2 µL pUC19 and a negative control with no plasmid DNA were also used. These were transferred to electroporation cuvettes, electroporated at 2500 V and immediately transferred to 5 mL prewarmed LB before incubation at 37°C with aeration for 1 hour. Cultures were then centrifuged, resuspended and plated on LB agar (LBA) with 100 µg/mL chloramphenicol for selection of cells containing pNDM-HK *gfp cat* and

50 µg/mL ampicillin for selection of cells containing pUC19. After 12 hours colonies were counted and tested by PCR for plasmid presence.

2.3.3 Transfer of pNDM-HK *gfp cat* by Filter Conjugation

Overnight cultures of donor (*E. coli* SW105) and recipient (*E. coli* ST131 EC958c and *E. coli* ST131 B104) strains were adjusted to OD_{600} 0.5 nm in LB. Donor to recipient ratios 1:4, 1:1 and 4:1 were tested, 100 µL of each was pipetted onto a sterile Whatmann filter disc and incubated on LBA at 30°C overnight. Cells from the filter disc were re-suspended by vortexing in 1 mL LB and serial dilutions spread on LB with 100 µg/mL chloramphenicol and 100 µg/mL rifampicin to select for transconjugants. Colonies were replica plated and tested by PCR for the presence of plasmid and *E. coli* SW105 DNA.

2.3.4 Detection of pNDM-HK *gfp cat* by polymerase chain reaction (PCR)

Colony PCRs were used for detection of pNDM-HK *gfp cat* with primers specific for the overlap of the *gfp* insert with the plasmid and IncL/M specific primers. The *gfp* primers were designed for this project and IncL/M primers had been previously described by Carattoli et al (46). PCRs were also performed with primers specific for an *E. coli* SW105 chromosomal gene to check the identity of colonies after filter conjugation. All primers and annealing temperatures are shown in Table 3.

DNA lysate for colony PCR was prepared by addition of the colony to be tested to 50 µL sterile water, before boiling at 100°C for 10 minutes and centrifugation at 13'000 x g for 2 minutes. 2.5 µL supernatant was added to each PCR reaction as shown in Table 4. PCR products were confirmed using agarose gel electrophoresis with a 1 kilobase (kb) DNA ladder (Bioline) used for confirmation of the size of PCR products.

Table 3. Primers used in this study

Name	DNA sequence (5' to 3')	Amplimer size	Annealing temperature (°C)	Description	Source
gfp in pNDM-HK	F CAACCATTACCTGTCCACAC R CAGCTCAACAGTCACACATAG	494	52	Amplification of *gfp* insert in pNDM-HK	Sigma
IncL/M check pNDM-HK	F GGATGAAAACTATCAGCATCTGAAG R CTGCAGGGGCGATTCTTTAGG	785	52	Amplification IncL/M backbone gene	Sigma
SW105 chromosomal gene	F GCGTCTATTTATGTAGGATGAAAGG R CAATTCCTCTTCCTAGCTACTTTCA	732	51	Amplification of SW105 chromosomal gene	Invitrogen
Ecl8 *gyrA* 1	F ATACAGTAGAGGGATAGCGG R GCGTCCACTTCCACTTCC	779	48	Amplification of *gyrA* from *K. pneumoniae* Ecl8 nalR for sequencing	Invitrogen Sigma
Ecl8 *gyrA* 2	F CCATTATCAATGGCCGTCGC R TCAGTTCGATAATCGGGTCG	528	48		Sigma Invitrogen
Ecl8 *gyrA* 3	F CGTTGCGCTGGCCAACAT R GACGGCTGAACTCGGTCA	845	48		Sigma
Ecl8 *gyrA* 4	F AAGAGGGCGTCAACGTCTT R CCTCCCTTCTGTGCGATAT	747	48		Sigma
EC958c *rpoB* 1	F GGCATTGCGGAAAGTGT R CGATGTACTCAACCGGG	981	51	Amplification of *rpoB* in *E. coli* EC958c rifR for sequencing	Invitrogen
EC958c *rpoB* 2	F CGCATCTTTTGACATCGA R TTGTGCGTAATCTCAGACAG	832	46.3		
EC958c *rpoB* 3	F ACGCACAAACGTCGTATC R GTTGTAACCATTCCACGG	861	48.3		
EC958c *rpoB* 4	F TCAGAACATGCGCGTAG R GTAAGGCATATCTTCGATCG	871	46.3		
EC958c *rpoB* 5	F CGGTAACAAGGGTGTAATTT R GCGAAGCCAGAGCAATT	974	47.2		
EC958c *rpoB* 6	F CGCATCTTTTGACATCGA R GTTGTAACCATTCCACGG	1684	47		

Table 4. PCR reaction mix

Reagent	Volume (µL)	Source
MyTaq Red Master Mix	12.5	Bioline
Forward primer (25µM)	1	See supplementary Table 1
Reverse primer (25µM)	1	
Template DNA	2.5	N/A
PCR grade water	8	Sigma

2.3.5 Generation of *K. pneumoniae* Ecl8 *mcherry* nal^R and *E. coli* EC958c *mcherry* rif^R

Overnight cultures (100 µL) of Ecl8 *mcherry* and EC958c *mcherry* were spread onto LBA supplemented with antibiotic (100 µg/mL rifampicin for EC958c and 64 µg/mL nalidixic acid for Ecl8) and incubated overnight at 37°C. In order to

calculate the mutation frequency, overnight culture was serially diluted (10^{-6} to 10^{-8}) in phosphate buffered saline (PBS) (Sigma-Aldrich) and incubated at 37°C overnight. Colonies were counted and the mutation frequency was calculated using the following formula.

$$Mutation\ frequency = \frac{Number\ of\ mutant\ cells/ml}{Total\ number\ of\ cells/ml}$$

Velvet stamping was used to replica plate Ecl8 mutants onto LBA containing 128 µg/mL nalidixic acid. After negative results mutant selection was repeated with Ecl8 *mCherry* however overnight culture was spread directly onto LBA supplemented with 128 µg/mL nalidixic acid.

2.3.6 Broth minimum inhibitory concentration (MIC)

The MIC of rifampicin and nalidixic acid for the generated mutants was tested using the British Society of Antimicrobial Chemotherapy guidelines (47). Antibiotic was doubly diluted in iso-sensitest broth from 512 µg/mL to 0.5 µg/mL in a microtitre tray with one well containing no antibiotic. Overnight culture diluted 1:100 was added to each well and the plate incubated at 37°C for 18 hours. The MIC was determined as the lowest concentration at which growth was prevented.

2.3.7 Sequencing *gyrA* and *rpoB*

Colony PCRs were performed to amplify *gryA* from Ecl8 and *rpoB* from EC958c using high fidelity Myfi taq polymerase (Bioline) and primers shown in Table 3. PCR products were confirmed using agarose gel electrophoresis and the DNA concentration of PCR products quantified using a nanodrop spectrophotometer. For sequencing, 10 ng DNA was added to each reaction with 3 µL primer (1 µM) and made up to 10 µL with nuclease free water. Sequencing was performed using the Applied Biosciences (ABI 3730) sequencing platform (University of Birmingham DNA sequencing facility). The data was analysed using multiple sequence alignment tool Clustal Omega (48).

2.4 Results

2.4.1 Transfer of pNDM-HK *gfp cat* into clinically relevant hosts by electroporation

pNDM-HK *gfp cat* from *E. coli* SW105 was electroporated into *E. coli* DH10B, this is a cloning strain used for storage of plasmids. Colonies were seen on selection plates with 100 µg/mL chloramphenicol after incubation for 24 hours. For all experiments pUC19 was also transformed to ensure cell competency and colonies were seen on plates supplemented with 50 µg/mL ampicillin. As a negative control no plasmid DNA was electroporated to one aliquot of cells and no colonies were seen on selection plates. Transformed DH10B colonies from chloramphenicol selection plates were replica plated and tested by colony PCR for plasmid presence. All colonies displayed presence of the *gfp* insert but no amplification of the IncL/M plasmid backbone gene (Figure 3). For all PCRs *E. coli* SW105 was tested as positive control and both *gfp* insert and IncL/M backbone gene amplified (Figure 3).

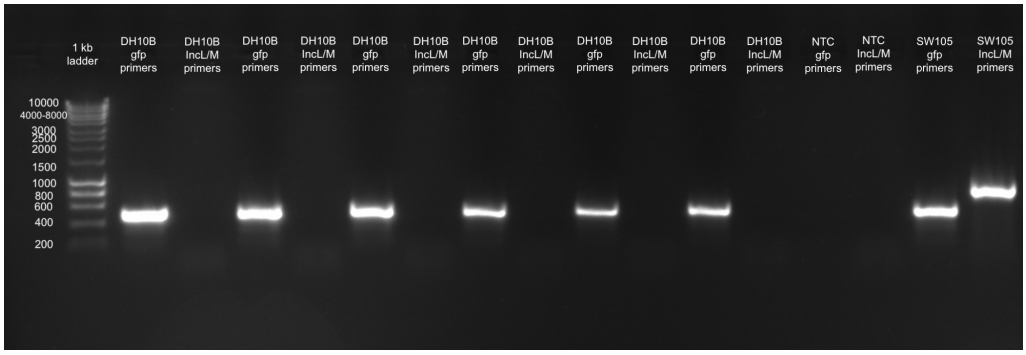


Figure 3. Agarose gel to check the presence of pNDM-HK *gfp cat* in electroporated *E. coli* DH10B cells. This gel shows 6 colonies of DH10B which were resistant to chloramphenicol and were tested by colony PCR for plasmid presence. The numbers on the left represent the size of each of the bands of the 1 kb ladder in base pairs. The gel shows amplimers indicating the presence of *gfp* insert in the plasmid (494 bp) with bands at ~500 bp for all colonies of DH10B and the positive control SW105 (far right). No bands are seen for any of the DH10B cells with primers specific for the IncL/M backbone however a band is seen for the positive control SW105 at ~800 bp representing the 794 bp fragment. No bands are seen in negative no template controls (NTC).

Plasmid DNA was extracted from transformed DH10B colonies and tested by PCR in case chromosomal DNA or cell debris from the cell lysates prepared for colony PCR interfered with the reaction. This also showed presence of *gfp* insert but not IncL/M backbone (data not shown). Electroporation was repeated into DH10B cells with the same result. Therefore, transformation of pNDM-HK *gfp cat* into a different *E. coli* strain, ST131 EC958c, was performed. Again, colonies showed the presence of *gfp* but not the IncL/M backbone gene when tested by PCR with SW105 tested as positive control showing amplification in both genes.

Electroporation of pNDM-HK *gfp cat* into two *E. coli* strains was unsuccessful therefore electroporation into *K. pneumoniae* Ecl8 was attempted to see if the result was *E. coli* specific. This gave the same result with colonies growing on chloramphenicol and *gfp* insert amplified but not the plasmid backbone gene.

2.4.2 Transfer of pNDM-HK *gfp cat* into clinically relevant *E. coli* strains by filter conjugation

Transformation of pNDM-HK *gfp cat* into clinically relevant strains by electroporation was unsuccessful therefore filter conjugation was attempted. *E. coli* SW105 was used as plasmid donor and *E. coli* strains ST131 B104 rif^R and ST131 EC958c rif^R nal^R were recipients. Different donor recipient ratios were tested to optimise transmission. Transconjugants were selected on plates containing rifampicin and chloramphenicol (Table 5). These were replica plated and tested by PCR for plasmid presence. All colonies showed presence of *gfp* insert and IncL/M backbone verifying the presence of pNDM-HK *gfp cat.* These colonies were then tested with primers specific for an SW105 chromosomal gene which showed that all apparent transconjugants were SW105 which had mutated to develop rifampicin resistance. ST131 B104 and EC958c were tested with SW105 gene primers and no fragment was amplified in either.

Table 5. Colonies seen on selection plates after filter conjugation with *E. coli* SW105 as plasmid donor

Recipient bacteria	Donor:Recipient Ratio	Colonies seen
E. coli ST131 EC958c	4:1	1
E. coli B104	1:1	2
E. coli B104	4:1	1

Filter conjugation was repeated with an increased concentration of rifampicin on selection plates (150 μg/mL) for selection of B104 transconjugants. ST131 EC958c is also resistant to nalidixic acid therefore 100 μg/mL nalidixic acid was added to selection plates for EC958c transconjugants. Increasing the concentration of antibiotic and adding a second antibiotic should reduce the ability of SW105 mutants to grow. SW105 mutants were seen again on plates with 150 μg/mL rifampicin (confirmed by PCR) and no colonies were seen on plates with rifampicin and nalidixic acid. In summary, pNDM-HK *gfp cat* was unable to be moved into *E. coli* DH10B, ST131 EC958c, B104 or *K. pneumoniae* Ecl8 using either electroporation or conjugation.

2.4.3 Generation of *mCherry E. coli* and *K. pneumoniae* mutants and sequencing

In order to enable selection of transconjugants after mating pCT *gfp* and pKpQIL *gfp* with strains expressing *mCherry* unique antibiotic resistance mutations were generated creating *E. coli* EC958c resistant to rifampicin (rif^R) and *K. pneumoiae* Ecl8 resistant to nalidixic acid (nal^R). The frequency of mutation when generating *E. coli* rif^R mutants was 3.06×10^{-8} and when generating *K. pneumoniae* nal^R mutants was 3.5×10^{-8}. The MIC of these mutants was tested, and the results shown in Table 6.

Nalidixic acid inhibits DNA synthesis by binding and inhibiting DNA gyrase and mutations in *gyrA* lead to resistance therefore this gene was sequenced from Ecl8 *mcherry* nal^R (49). Rifampicin inhibits RNA polymerase and resistance is due to mutations in the β-subunit of RNA polymerase (*rpoB*) so *rpoB* was sequenced from EC958c *mcherry* nal^R (50). The strains with the highest MIC

were sequenced, this was strain 1 for *E. coli* and strain 4 for *K. pneumoniae* from Table 6.

Table 6. MIC of rifampicin and nalidixic acid for mutants generated.

Compound	Strain	MIC (µg/mL)
Rifampicin	*E. coli* EC958c *mcherry* rif^R (1)	>512
	E. coli EC958c *mcherry* rif^R (2)	>512
	E. coli EC958c *mcherry* rif^R (3)	256
Nalidixic acid	*K. pneumoniae* Ecl8 *mcherry* nal^R (1)	512
	K. pneumoniae Ecl8 *mcherry* nal^R (2)	512
	K. pneumoniae Ecl8 *mcherry* nal^R (3)	512
	K. pneumoniae Ecl8 *mcherry* nal^R (4)	512
	K. pneumoniae Ecl8 *mcherry* nal^R (5)	256

PCRs with 4 primer pairs were performed for sequencing of *gyrA* (Figure 4) however no mutations were found compared to wild-type. Three further colonies were sequenced but still no mutations found. Mutant selection was repeated and Ecl8 was spread onto LBA with nalidixic acid at 128 µg/mL rather than 64 µg/mL. 3 colonies grew and *gryA* was sequenced from each of these, but no mutations were found.

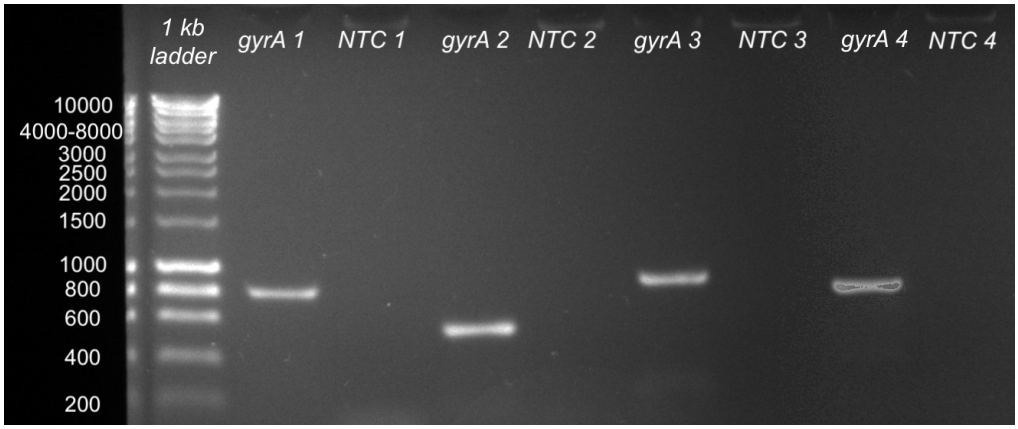


Figure 4. Agarose gel of PCR products amplifying *gyrA* in Ecl8 *mcherry* nal^R for DNA sequencing. PCRs were performed with 4 sets of primers designed to cover the whole gene. The numbers on the left represent the sizes of the bands of the 1 kb ladder in base pairs. The bands represent PCR products from each primer pair with NTCs for each primer pair also shown. Bands are seen at ~780, 530, 850 and 750 bp. PCR products were purified and sequenced.

PCRs were performed with 6 primer pairs for sequencing *rpoB*. A single point mutation in nucleotide 1598 was found substituting cysteine with thymine (Figure 5) changing amino acid 533 from serine (TCT) to phenylalanine (TTT). This was the only mutation and was concluded to be the cause of rifampicin resistance in this strain.

```
WT      CAGGATATGATCAACGCCAAGCCGATTTCCGCAGCAGTGAAAGAGTTCTTCGGTTCCAGC   1560
rpoB    CAGGATATGATCAACGCCAAGCCGATTTCCGCAGCAGTGAAAGAGTTCTTCGGTTCCAGC   1560
        ************************************************************

WT      CAGCTGTCTCAGTTTATGGACCAGAACAACCCGCTGTCTGAGATTACGCACAAACGTCGT   1620
rpoB    CAGCTGTCTCAGTTTATGGACCAGAACAACCCGCTGTTTGAGATTACGCACAAACGTCGT   1620
        ********************************** **********************

WT      ATCTCGGCACTCGGCCCAGGCGGTCTGACCCGTGAACGTGCAGGCTTCGAAGTTCGAGAC   1680
rpoB    ATCTCGGCACTCGGCCCAGGCGGTCTGACCCGTGAACGTGCAGGCTTCGAAGTTCGAGAC   1680
        ************************************************************
```

Figure 5. Sequencing data from *rpoB* from *E. coli* EC958c *mcherry* nal^{R}. The sequence of *rpoB* from the mutant (bottom, rpoB) aligned with the wild type (top, WT). A segment of the sequencing data showing the mutation in codon 533 changing TCT to TTT coloured in red is shown.

2.5 Discussion

2.5.1 Transfer of pNDM-HK *gfp cat* into *E. coli* and *K. pneumoniae*

Transfer of pNDM-HK *gfp cat* into *E. coli* and *K. pneumoniae* by both electroporation and conjugation was unsuccessful. After electroporation all recipient cells showed the presence of *gfp* insert and cells grew on LBA with chloramphenicol. This implies plasmid DNA was transferred to recipient cells however no fragments corresponding to the IncL/M backbone gene were amplified. Ho et al. sequenced pNDM-HK and discovered mobile genetic elements including an IS*26* transposon flanking *bla*$_{\text{NDM-1}}$. These may enable the fragment located within the transposon to insert into the chromosome (31). In the pNDM-HK *gfp cat* plasmid construct, *gfp* and *cat* were inserted adjacently in the place of *bla*$_{\text{NDM-1}}$ therefore these genes were flanked by IS*26*. Although Ho et al. did not see chromosomal insertion of *bla*$_{\text{NDM-1}}$, IS*26* has been shown to lead to insertion of *bla*$_{\text{CTX-M}}$ in *E. coli* isolates (31, 51). This implies *gfp* and *cat* may have integrated into the recipient cell chromosome, enabling the cell to survive on chloramphenicol supplemented media while losing the plasmid

backbone. Kottara et al. studied movement of plasmid pQBR103 in *Pseudomonas* strains, they displayed that the mercury resistant phenotype encoded on the plasmid was present even after loss of the plasmid. They concluded that the mercury resistance gene integrated into the chromosome and the redundant plasmid was lost (52). This may have been the case with pNDM-HK *gfp cat* as beneficial genes from the plasmid integrate into the host chromosome (53). The chromosome of recipient cells could be sequenced to confirm this.

As electroporation was unsuccessful filter conjugation was attempted however no transconjugants were seen. This could be due to the large size of the plasmid (88 kb) which may mean that transmission is less efficient. However, this is unlikely as Ho et al. saw high conjugation frequencies of pNDM-HK into *E. coli* J53. They saw conjugation frequencies ranging from 10^{-8} to 10^{-3} transconjugants per donor cell with increased conjugation at lower concentrations of antibiotic, therefore differing antibiotic concentrations could be used here in order to promote conjugation (31). Additionally, they performed conjugation assays with the plasmid carrying bla_{NDM} whereas here the gene is replaced with *gfp* and *cat*, this could affect the conjugation frequency. Conjugation of pNDM-HK *gfp cat* should be attempted into *E. coli* J53 to determine if the insertion of *gfp cat* is affecting conjugation or whether it is the specific strains tested.

In order to transform clinically relevant strains with pNDM-HK *gfp cat* to use as plasmid donors in conjugation experiments, attempts could be made to optimise the electroporation or filter conjugation assays. Filter conjugation could be attempted with an increased incubation time at 30°C, this is the optimal temperature for donor cell growth but not recipients. The slower growth of recipient cells may mean conjugation occurs at a lower rate therefore increased incubation times may increase the likelihood of plasmid transferring. Plasmid conjugation has been shown to occur at a higher rate when cells are in exponential growth (33). Therefore, the assay could be

optimised to ensure the cells are in this growth phase to promote plasmid transfer.

Conjugation assays may not have worked due to restriction modification systems present in recipient cells. Restriction modification involves recognition and cleavage of foreign, unmethylated DNA causing its degradation. The EcoKI type I restriction modification system in *E. coli* has been shown to affect the uptake of foreign DNA by conjugation (54). This could be inhibiting the transfer of pNDM-HK to *E. coli* strains via filter conjugation. The restriction modification genes can be knocked out to determine if these are affecting conjugation.

In *E. coli* EC958c and *K. pneumoniae* Ecl8 conjugation and maintenance of pCT and pKpQIL is seen however this is not seen with pNDM-HK in these strains. The differences between these plasmids could be investigated further to identify why pCT and pKpQIL are maintained and pNDM-HK is not. Additionally, the sequence of *E. coli* J53 and the strains used here could be compared. Ho et al. saw high conjugation frequencies of pNDM-HK into this strain therefore comparison of the genome could identify features of *E. coli* ST131 EC958c and B104 which may prevent conjugation of the plasmid.

Once the plasmid has been transferred into a clinically relevant strain it would be possible to measure its transmission using the flow cytometry-based assay established in the lab. Broth mating experiments will be set up with the pNDM-HK donor strain and other clinical strains as recipients. The rate of transfer of this plasmid will be determined into different recipients. When this assay is established to optimise conjugation, potential inhibitors will be screened, and inhibition will be measured via flow cytometry. This will identify conjugation inhibitors which can be used in combination with antibiotics to help prevent the spread of AMR genes.

2.5.2 Generation of *E. coli mcherry* and *K. pneumoniae mcherry* mutants

K. pneumoniae Ecl8 *mcherry* and *E. coli* EC958c *mcherry* with unique antibiotic resistance mutations were generated and specific genes sequenced in order to

define the mutations leading to resistance. In *K. pneumoniae* Ecl8 *mcherry* nal^R, *gyrA* was sequenced. Mutations in this gene, usually point mutations in the quinolone resistance-determining region, prevent fluoroquinolones such as nalidixic acid binding to DNA gyrase A so lead to resistance (49, 55, 56). In total 7 mutants were sequenced however no mutations were found in *gyrA* for any of these indicating mutations in a different gene are responsible for nalidixic acid resistance. As well as mutations in *gyrA,* mutations in parC, a component of topoisomerase IV can lead to fluoroquinolone resistance although mutations in this gene are usually seen in conjugation with mutations in *gryA* (56). Additionally, mutations causing overexpression of *ramA*, a transcriptional activator involved in multidrug resistance can result in nalidixic acid resistance through antibiotic efflux (57). Loss of outer membrane porin OmpK35 has also been reported to contribute to nalidixic acid resistance (58). In order to determine the mutation causing nalidixic acid resistance in these strains it would be best to sequence the whole genome. Once the mutation is confirmed the next step would be to mate this strain with pKpQIL *gfp*. This can be used as plasmid donor to non-fluorescent cells to measure plasmid transmission in multi-species environments.

E. coli EC958c *mcherry* rif^R had a single point mutation in codon 533 of *rpoB*, the ß-subunit of bacterial RNA polymerase, changing it from serine to phenylalanine. This mutation will impair rifampicin binding leading to resistance as serine is a polar, uncharged amino acid whereas phenylalanine is hydrophobic (50). Mutations in this section of the gene have been reported previously to confer rifampicin resistance and it is thought that mutations at a secondary site are possible but unlikely (59, 60). This mutation was concluded to be the cause of rifampicin resistance.

The next step with this strain would be to inactivate aminoglycoside 3'-phosphotransferase (*aph*) in the chromosome which confers kanamycin resistance. pCT contains *aph* for selection therefore inactivation of this in the chromosome is essential for selection of transconjugants. This can be performed using lambda red recombination (61). *aph* is flanked by FRT sites

which are recognised by a recombinase encoded on plasmid pCP20 which can be transferred to *E. coli* cells by electroporation. This procedure was initiated during this project. Once *aph* is inactivated, the strain can be mated with pCT *gfp* and used as plasmid donor strain.

E. coli EC958c *mcherry* rif^R pCT *gfp* and *K. pneunomiae* Ecl8 *mcherry* nal^R pKpQIL *gfp* will then be used in conjugation assays as plasmid donors to unmodified bacteria in multispecies environments. Recipient cells will fluoresce green on acquisition of the plasmid and their identity can be confirmed by microscopy or through use of fluorescence activated cell sorting. This will mimic transmission of plasmids in clinical settings with mixed bacterial species and inhibitors of conjugation can be tested in these environments.

3 Developing Tools to Investigate *Staphylococcus aureus* Biofilm Growth

3.1 Abstract

Staphylococcus aureus biofilm growth makes infections hard to treat and limits the efficacy of drugs meaning that infections are not cleared. Cells in a biofilm are tolerant to higher concentrations of antibiotics than planktonic cells, this leads to increased hospital stays and morbidity. The aim of this project was to validate tools in the lab which will be used to monitor *in vivo* infection sites. Investigation of *S. aureus* biofilms will enable improvement of strategies for tackling them and will help discovery of new drug targets. Phenotypic analysis was performed with bioluminescent strains of *S. aureus* visualised using confocal microscopy. Biofilms were grown on beads and the biomass of each biofilm calculated; beads were used to remove the bias seen when visualising biofilms *in vitro.* Ceramic beads were used as tooth models and cytodex beads used as these are used as supports *in vivo* in virulence models. Biofilms were grown in saliva media to replicate oral biofilm growth and differences in biofilm establishment were seen on each bead, more biofilm biomass was seen in 10% TSB than saliva media on ceramic beads and more biomass in saliva media than 10% TSB on cytodex beads. A strain with deletion of the *agr* system was also tested and this showed increased biofilm biomass compared to wild type under all conditions. Creation of a strain with knockout of a novel regulator of *agr* was initiated which will be used to determine the role of this regulator in biofilm growth. Additionally, dyes were used successfully to stain cells undergoing cell division, protein synthesis and active metabolism in the biofilm. These can be used to discover novel antibiotic targets in the biofilm.

3.2 Introduction

Staphylococcus aureus (*S. aureus*) has been recognised by the World Health Organisation as a high priority pathogen (22). *S. aureus* is a Gram-positive

bacteria which colonises around 30% of the population and is a common cause of nosocomial infections (62, 63). Infections caused by *S. aureus* are difficult to treat due to the emergence of drug resistant strains and growth in biofilms which limits the efficacy of drugs leading to longer hospital stays and increased mortality rates (64). *S. aureus* causes acute infections such as bacteraemia as well as chronic infections such as osteomyelitis and endocarditis (65). It is estimated 80% of chronic *S. aureus* infections are associated with biofilm growth (66). Biofilms can form on artificial and tissue surfaces such as implanted medical devices or the oral cavity causing persistent infections (62, 67).

Biofilms are heterogeneous, sessile communities of bacterial cells encased in a matrix of extracellular polymeric substance consisting of DNA, protein and polysaccharide (62). They form on artificial and tissue surfaces such as implanted medical devices or the oral cavity causing persistent infections which are difficult to cure (62, 67, 68). Biofilm growth allows bacteria to persist *in vivo* by resisting host clearance mechanisms and displaying increased tolerance to antibiotics (67). This is thought to be due to the presence of metabolically inactive cells which are tolerant to high antibiotic concentrations and the slow diffusion of antibiotics through the biofilm matrix (12, 68, 69). Low oxygen and nutrient levels in the biofilm produce populations of cells with low metabolic activity which provides resistance to antibiotics. For example, cells with low protein synthesis activity will not be affected by aminoglycoside antibiotics and cells with low DNA synthesis activity will be more resistant to quinolones. These are different to persister cells, also present in the biofilm which are metabolically inactive due to bacterial differentiation into a dormant state (67). After antibiotic treatment has ended, metabolically inactive cells are often not cleared and can return to the active state and re-establish infection (69). Additionally, cells can seed off from the biofilm and set up infections at secondary sites in the body meaning infections are not cleared (12, 70). Understanding the mechanisms involved in biofilm establishment, survival and tolerance of antimicrobials will enable development of treatments against

these persistent infections (67). The aim of this project is to develop tools for the improved identification of antimicrobial targets in *S. aureus* biofilms.

S. aureus biofilm growth involves three main stages; attachment, maturation and dispersal, these involve up and downregulation of specific genes controlled in the biofilm by quorum sensing (70, 71). Understanding these processes should lead to the development of new biofilm control strategies (71). Staphylococci have two quorum sensing systems, the luxS and the accessory gene regulator (*agr*) systems. LuxS is involved in cell to cell adhesion and *agr* plays a role in biofilm growth as well as having a key role in virulence regulation (72-74). The *agr* system is outlined in Figure 6. *agr* expression is associated with the dispersal of cells from biofilms due to upregulation of detergent-like peptides (65, 74). Downregulation or loss of *agr* leads to growth of thicker biofilms due to the inability of cells to detach from the biofilm (66, 75, 76). *agr* is important in switching between planktonic and biofilm growth as its downregulation is essential for biofilm formation and reactivation of the system activates cell dispersal (66). A *S. aureus* strain with deletion of *agr* was tested in biofilm models to see the effect of this deletion on biofilm biomass.

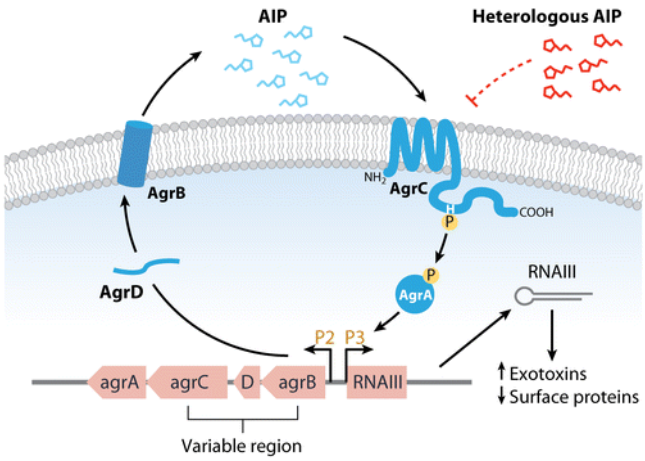


Figure 6. Outline of the *agr* system in *S. aureus* (77). Promotors P2 and P3 induce production of RNAII and RNAIII (78). This induces a positive feedback loop causing continual upregulation of RNAII and RNAIII through production of the pheromone autoinducing peptide (AIP) (77, 79). Upregulated RNAIII increases transcription of several secreted virulence factors giving *agr* its role in staphylococcal pathogenesis (65, 78).

Inhibition of the *agr* system is an interesting therapeutic target as interfering with this system could reduce the virulence of *S. aureus* and make the infection easier to control (80). Quorum sensing inhibitors can be used in combination with traditional therapies as they can increase bacterial sensitivity to antibiotics (81). However it has been shown that in some infections *agr* deficient bacteria are present, these are present in high numbers in cases of bacteraemia and will mean quorum sensing inhibitors have no effect (80). Additionally inhibition of the *agr* system will increase biofilm formation which can make infections harder to clear (66).

There are many regulators involved in the *agr* system such as SarA and SarR (80). Recently a putative protease located close to the *agr* operon on the chromosome known as SAUSA300_1984 (1984) or MroQ has been discovered. This is a transmembrane protein conserved across staphylococcal species involved in quorum sensing and it is thought to be necessary for *agr* function (82). The role of this gene in regulation of the *agr* system is being investigated and one of the objectives of this study was to knock out 1984 to enable study of its role in biofilm growth.

S. aureus has been isolated from oral biofilms and saliva of healthy individuals. As staphylococci are commonly present in the nasal flora it is thought they can pass from here to the mouth (83). Oral carriage of *S. aureus* has been shown to range from 24-36% in healthy adults (84). It is thought the mouth could be a reservoir for staphylococci which can cause infection when there is a breakdown in the oral cavity (84, 85). *S. aureus* has a strong association with dental implant infections (85). This can lead to systemic and chronic infections which establish at secondary sites as cells seed off from biofilms (70, 84, 85). Therefore, prevention of biofilm growth in the mouth could improve patient health. In this study ceramic beads will be used as a model for biofilm growth on teeth in artificial saliva media.

Development of novel methods for monitoring biofilms and host responses to biofilm infections will help development of therapeutics. It is recognised that

biofilm models grown *in vitro* cannot entirely replicate growth *in vivo* however they provide simplified, basic models which can be used for screening prior to *in vivo* work and which generally mimic the main hallmarks of biofilm biology (86). *In vitro* models can be used to study the role of genes in biofilm formation and regulation and for screening of antimicrobial agents however do not take into account environmental or host factors (86). *In vitro* biofilms are limited due to the inability to replicate the host environment as *in vivo* biofilms can be variable depending on the site of infection (67, 86). The complexity of biofilms *in vivo* is increased due to the heterogeneity of biofilm-forming clinical strains which may have different gene expression patterns due to adaptation during chronic infection (67). Some strains may show poor biofilm formation *in vitro* but grow biofilm well *in vivo* (86). *In vivo* biofilms are usually polymicrobial therefore it is important to study polymicrobial biofilms *in vitro* to mimic the clinical environment. Study of polymicrobial biofilms and improvement of *in vitro* models will help to identify molecular mechanisms of biofilm growth and bacterial interactions which will ultimately lead to identification of molecules to inhibit these and target these biofilms (86). The aim of this project was to develop tools for investigation of *S. aureus* biofilms.

Use of bioluminescent strains enables monitoring of biofilm development and bacterial burden and responses to antibiotic treatment (87-89). Here strains expressing a *Photorhabdus luminescens*-modified *lux* operon (*luxA* to *luxE*) were used which emit a constitutive bioluminescent signal when the bacteria is metabolically active (88, 90). These strains are used in infection models *in vivo* therefore biofilm growth with these strains was monitored *in vitro* modelling the clinical infection site. One of the objectives of this study was to generate a bioluminescent clinical *S. aureus* strain using USA300 JE2 to be used as a reporter strain in infection and biofilm models *in vitro* and *in vivo*.

S. aureus biofilm growth was compared on ceramic and cytodex beads in artificial saliva media. Ceramic beads were used to mimic the interaction with tooth enamel and cytodex beads were used to validate these supports which are used *in vivo* in virulence models. Cytodex beads are injected in murine

models as supports for biofilm growth mimicking medical implants such as hip replacements or catheters on which biofilm forms clinically (62). Beads were used as biofilm supports to remove bias in biofilm imaging as a defined number of beads were imaged per experiment. Preliminary *in vivo* virulence testing was also performed in *Galleria melonella* infection models.

This project aimed to develop phenotypic screens for the characterisation of *S. aureus* strains and determination of new virulence targets. Biofilms are complex and heterogeneous as cells migrate to optimal positions for access to light, nutrients, metabolites and signalling molecules. Even in monospecies biofilms heterogeneity is seen as cells adapt to their environment (91). Confocal laser scanning microscopy (CLSM) was used to monitor cell activities with markers for protein synthesis, metabolism and cell division (91). 'Click' chemistry was used where molecules form covalent bonds with biomolecules and can be detected with fluorescent azides (92, 93). Use of these dyes enables determination of the spatial arrangement of cells in the biofilm (91).

3.3 Methods

3.3.1 Bacterial strains and growth media used

Bacterial strains used are outlined in Table 7. *E. coli* strains carrying pIMAY were grown at 30^{o}C, all other strains were grown at 37^{o}C. Overnight cultures were grown with aeration by shaking at 200 rpm.

Table 7. Bacterial strains used in this study.

Strain	Description	Antibiotic resistance	Use
S. aureus SH1000 lux	SH1000 strain expressing lux cassette from Xen29	Kanamycin (50 µg/mL)	Biofilm models
S. aureus SH1000 lux SNAP	SH1000 strain expressing lux with SNAP tag linked to sortase	Kanamycin (50 µg/mL)	Biofilm models
S. aureus Xen29	Reporter strain expressing lux operon from *Photorhabdus luminescens* (88).	Kanamycin (50 µg/mL)	Biofilm models
S. aureus Xen SNAP	Xen29 expressing lux operon with a SNAP tag linked to sortase	Kanamycin (50 µg/mL)	Biofilm models
S. aureus Xen Δ*agr*	*S. aureus* Xen9 with deletion of *agr*	N/A	Biofilm models
S. aureus USA300 JE2	Methicillin resistant clinical strain	N/A	Recipient in phage transduction experiments to be transduced with lux cassette
S. aureus USA300 JE2 lux	Clinical strain expressing lux	Kanamycin (50 µg/mL)	Created in this study for use in future phenotypic models
E. coli DC10B	Cloning strain	N/A	Recipient of pIMAY 1984 construct
E. coli DH5α	Strain carrying plasmid pIMAY	Chloramphenicol (10 µg/mL)	pIMAY donor
E. coli mach1	Strain carrying plasmid pUNK	Erythromycin (150 µg/mL)	pUNK donor used for amplification of erythromycin resistance gene

3.3.2 Growth media

Staphylococci were cultured in tryptone soy broth (TSB) (Oxoid) and *E. coli* in LB unless otherwise specified with antibiotics added as required. Kanamycin was sourced from Thermofisher and chloramphenicol and erythromycin from Sigma. Biofilms were grown in 10% TSB diluted in PBS or artificial saliva media 1. Artificial saliva media is detailed in Table 8.

Table 8. Components of artificial saliva media. Porcine stomach mucins and urea were added after autoclaving and the media filter sterilised. These were adapted from media used previously (94-96).

Reagent	Quantity (% w/v)	
	Artificial saliva 1	Artificial saliva 2
Porcine stomach mucins	0.25	0.25
Sodium chloride	0.35	0.035
Potassium chloride	0.02	0.02
Calcium chloride dihydrate	0.02	0.02
Yeast extract	0.2	0.2
Beef extract	0.1	0.1
Proteose peptone	0.5	0.5
Urea	0.05	0.05
dH_2O	To required volume	To required volume

3.3.3 Generation of phage lysate and phage transduction

Overnight culture of *S. aureus* SH1000 lux was grown in LK broth and 0.5 mL added to 5 mL phage buffer and 5 mL LK broth with phage at volumes of 0, 10, 50 and 100 µL. Reactions were incubated statically at 37°C until the solutions became clear then passed through a 0.2 µM filter and stored at 4°C.

For transduction *S. aureus* JE2 was grown overnight in LK broth and 0.5 mL added to 1.5 mL LK broth with 10 mM $CaCl_2$ and volumes of phage lysate; 0 µl, 100 µL and 200 µL. Reactions were incubated statically at 37°C for 25 minutes and then with shaking at 200 rpm for 15 minutes. 1 mL ice cold 20 mL trisodium citrate was added and the reactions incubated on ice for 5 minutes before centrifugation at 7600 x g and resuspension in 1 mL 20 mM trisodium citrate. Reactions were incubated on ice for 4-5 hours, centrifuged and resuspended to 500 µL. This was spread over 5 tryptic soy agar (TSA) plates with 20 mM trisodium citrate and 100 µg/mL kanamycin with 100 µL on each plate. Plates were incubated at 37°C overnight. Colonies seen were re-streaked and bioluminescence visualised.

3.3.4 MIC

The MIC of oxacillin for the JE2 lux strains was tested. Oxacillin (Sigma) was doubly diluted in Mueller Hinton broth (MHB) (Oxoid) from 64 µg/mL to 1 µg/mL in a microtitre tray. Overnight culture diluted 1:1000 was added and the

plate incubated at 37°C for 18 hours. The MIC was determined as the lowest concentration at which growth was prevented.

3.3.5 Generation of allelic exchange vector

pIMAY was used as allelic exchange vector for knockout of 1984 in *S. aureus* SH1000 and replacement of the gene with an erythromycin resistance gene (*erm*) through homologous recombination as outlined in Figure 7. pIMAY and pUNK were extracted using GenElute Plasmid miniprep kit (Sigma) from *E. coli* DH5α and *E. coli* mach1 respectively. Genomic DNA was extracted from *S. aureus* SH1000.

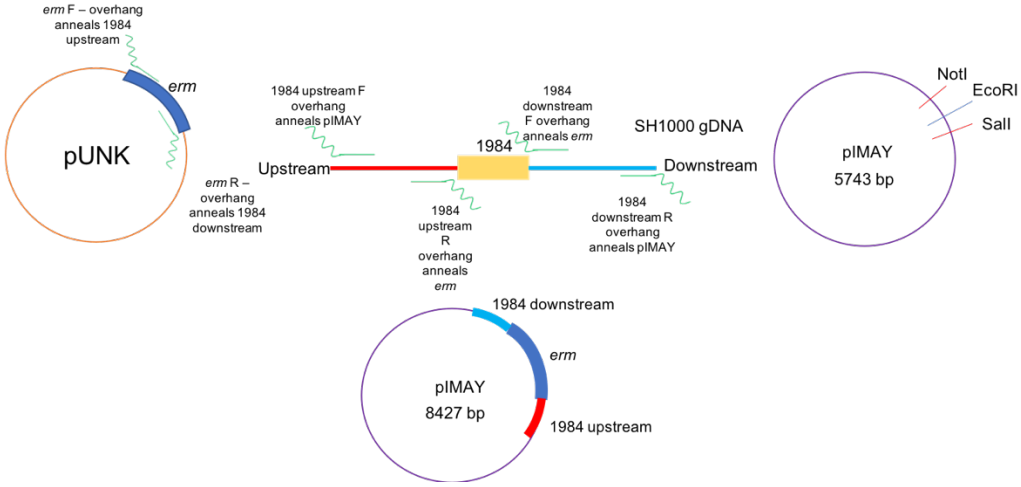


Figure 7. Strategy for creation of recombinant pIMAY to use in allelic exchange. Recombinant pIMAY contained 843 bp upstream of 1984 from SH1000, *erm* from pUNK and 844 bp downstream of 1984 from SH1000. Plasmid pUNK, SH1000 gDNA and pIMAY are shown with primers annotated. The fragments ligate into the multiple cloning site (MCS) of pIMAY.

Fragments were amplified from pUNK and SH1000 genomic DNA by PCR with Q5 DNA polymerase (NEB) and primers shown in Table 9. PCR primers were designed with overhangs to enable annealing of fragments (shown in Figure 7). pIMAY was digested with NotI-HF and SalI-HF (NEB), by incubation at 37°C for 2 hours and 65°C for 30 minutes to inactivate the enzymes. For ligation, PCR products and plasmid pIMAY were added at 0.2 pmol with Hifi DNA assembly mix (NEB) and deionised water and incubated at 50°C. 5 µL ligation product was electroporated into 60 µL electrocompetent *E. coli* DC10B cells.

Table 9. Primers used in this study

Name	DNA sequence (5' to 3')	Amplimer size (bp)	Overhang anneals to	Description
1984	F AGTCATGGATCCGATTGTTCCTCCTTAAAA	NA	NA	Binds in upstream region of 1984, used for sequencing
1984 upstream	F ctgggtaccgggccccccctcgaggGTCGTACCGTCACC AGCAATTTC	843	pIMAY	Amplification of 843 bp upstream of 1984 from SH1000 gDNA
	R aattcattcctggTGTCATAATTTTCCTCCAAATATTTG TTTATAATTTATTTTATCG		Erythromycin resistance gene	
Erythromycin	F gaaaattatgacaCCAGGAATGAATTACTATCCCTT TTATC	1165	1984 upstream region	Amplification of erythromycin resistance gene from pUNK
	R gttttttttattatggGACCTCTTTAGCTCCTTGGAAG		1984 downstream region	
1984 downstream	F agctaaagaggtcCCATAATAAAAAAAACGAATCAC	844	Erythromycin gene	Amplification of 844 bp downstream of 1984 from SH1000 gDNA
	R cgaattggagctccaccgcggtggcCTAATAAGCCAAATCC GGATC		pIMAY	

Electrocompetent cells were prepared by re-growth of overnight culture to OD_{600} 0.6 before cooling on ice and washing 4 times in ice cold 10% glycerol with final suspension in 1 mL 10% glycerol. After electroporation 1 mL LB was added and the cells incubated at 30°C with shaking for 1 hour before plating on LB with 10 µg/mL chloramphenicol and incubation at 30°C overnight for selection of colonies containing pIMAY.

Colony PCR was used to test for the presence of inserts using DreamTaq Green PCR mastermix (ThermoFisher) and primers in Table 9 (1984 upstream F and 1984 downstream R). Plasmids were digested with EcoRI-HF (NEB) in cutsmart buffer (NEB) at 37°C. Products were quantified on a 1% agarose gel by electrophoresis. Plasmids were sequenced by Source BioScience Sequencing, Nottingham.

pIMAY containing inserts was electroporated into *S. aureus* SH1000. Electrocompetent cells were created by re-growth to OD_{600} 0.4 and washing 4

times in 10% glycerol at room temperature with final suspension in 1 mL 10% glycerol. 5 µL plasmid was added to 60 µL electrocompetent cells and incubated at room temperature for 10 minutes prior to electroporation. After electroporation 3 mL brain heart infusion (BHI) broth was added and cells were incubated with shaking at 28^{o}C overnight. 100 µL was plated on BHI with 10 µg/mL chloramphenicol and incubated at 28^{o}C.

3.3.6 Growth curves

Overnight cultures washed in PBS were adjusted to OD_{600} 0.01 nm in TSB, artificial saliva 1 or artificial saliva 2. Each strain with each media was tested in triplicate, 200 µL was placed in a well of a 96 well plate. In a TECAN plate reader the OD_{600} and bioluminescence was recorded every 30 minutes for 16 hours.

3.3.7 Biofilm models

Cytodex beads (Sigma) were prepared by adding 0.5 g beads to 10 mL PBS. 1.4 mm ceramic beads and cytodex beads were autoclaved before use. In order to seed biofilms 6 ceramic beads or 20 µL cytodex beads were added to 1.5 mL eppendorf tubes with 1 mL overnight culture diluted in 10% TSB or artificial saliva 1 to OD_{600} 0.01. These were placed horizontally in a static incubator for 1.5 hours at 37^{o}C before removal of planktonic growth and transfer of beads to a 24 well microtitre plate (Thermofisher). 1 mL fresh media was added before overnight incubation.

After overnight incubation planktonic growth was removed and biofilms stained as outlined in Table 10. Biofilms were fixed with formal saline. Beads were imaged using a Zeiss LSM-700 laser scanning confocal microscope with the gain set the same for all images per experiment to remove bias.

Table 10. Biofilm fluorescent markers

Stain	Excitation (nm)	Emission (nm)	Concentration	Incubation	Function
FM1-43	485	610	0.05 µg/mL	20 minutes RT	Lipid stain which fluoresces when incorporated into the outer leaflet of the cell membrane (97).
FM4-64	515	740	0.05 µg/mL	20 minutes RT	Lipid stain which fluoresces when incorporated into the outer leaflet of the cell membrane.
EdU with Alexa Fluor 594	590	620	10 µM	1 hour 37°C Alexa fluor 594 30 minutes 37°C	Thymidine analogue incorporated to DNA during cell cycle to tag cell division detected using a click reaction with Alexa Fluor 594 (92)
OPP with Alexa Fluor 594	590	620	10 µM	1 hour 37°C Alexa fluor 594 30 minutes 37°C	Puromycin analogue forms covalent bonds with newly synthesised polypeptides for detection of protein synthesis. detected using a click reaction with Alexa Fluor 594 (93)
Calcein AM	485	530	10 µM	30 minutes 37°C	Converted to green fluorescent calcein when hydrolysed by intracellular esterases. Used to determine cell viability and metabolism (98).

3.3.8 *Galleria mellonella* infection models

Overnight cultures were washed 3 times in PBS, the OD_{600} corrected to 0.1 and diluted in PBS to 10^8, 10^7, 10^6 cfu/mL. The syringe used for injection was washed 3 times in 100% ethanol and PBS. 10 µL PBS as a control and each dilution was injected into the back left proleg of the worm, 5 worms were

injected per dilution. The wax worms were incubated at 37°C and alive worms counted at intervals up to 96 hours.

3.4 Results and Discussion

3.4.1 Phage transduction to create *S. aureus* JE2 lux

The phage used carried a lux operon (*luxA* to *luxE*) and kanamycin resistance gene. After transduction colonies seen on kanamycin selection plates were re-streaked and three showed bioluminescence. Two of the strains were closer in appearance to SH1000 while the other appeared more like USA300 (Figure 8). Therefore, the MIC of these strains against oxacillin was tested and compared to wild type JE2. The MIC of strains 1 and 2 (Figure 8) was <1 µg/mL for strain 2 was 16 µg/mL and for wild type JE2 was 8 µg/mL. This confirms strain 2 is USA300 JE2 expressing lux (JE2 lux). The MIC of JE2 with oxacillin has been reported to be 32 µg/mL (97). This is two-fold different than what is seen for JE2 lux, the difference could be due to the exact strains tested or pipetting differences. Sequencing would confirm this strain and the lux-kanamycin insertion site in the chromosome. This strain will be used in biofilm models *in vitro* and *in vivo*.

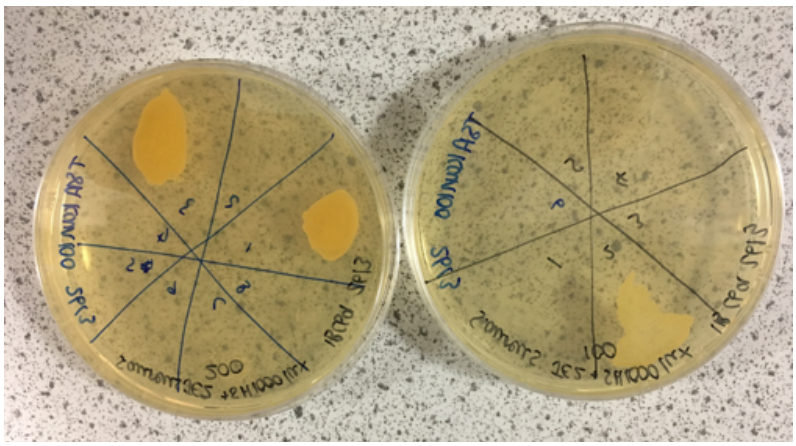


Figure 8. Plates showing the appearance of *S. aureus* strains which expressed bioluminescence after phage transduction

Phage transduction was also attempted with phage carrying the lux cassette, kanamycin resistance gene and SNAP. The SNAP tag is linked to sortase and presents on the exterior of the cell to enable detection with Alexa fluor azides.

No colonies were seen producing bioluminescence on selection plates therefore this would need to be repeated. The titre of the phage carrying the lux cassette, kanamycin resistance and SNAP tag should be calculated. This can be used to calculate the multiplicity of infection, the ratio of phage to bacteria, which can be used to optimise transduction. A higher ratio would be required as only one copy of the region to be inserted is carried per phage.

This method was used previously to create SH1000 lux and SH1000 lux SNAP strains used in this project.

3.4.2 Knockout of 1984 in *S. aureus* SH1000

pIMAY carrying chloramphenicol resistance was used as allelic exchange vector for knockout and replacement of 1984 with an erythromycin resistance gene (*erm*). pIMAY is temperature sensitive in staphylococci and replication is stimulated at 28°C. In order to induce integration of the plasmid into the chromosome, a single cross-over event is stimulated by growth at 37°C. The plasmid is then excised and yields the SH1000 chromosome with knockout of 1984 and replacement with *erm* (98). This is displayed in Figure 9.

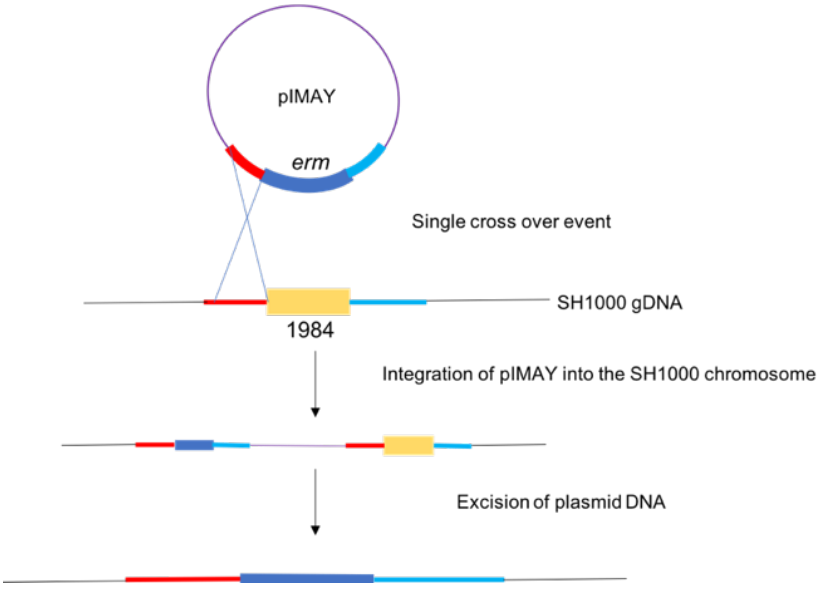


Figure 9. Schematic of allelic exchange with pIMAY

Recombinant pIMAY was created with an 843 bp region upstream from 1984, *erm* (1165 bp) and an 844 bp region downstream from 1984. These fragments

ligate into the MCS of pIMAY, replacing the EcoRI restriction site. PCRs were performed to amplify each fragment and pIMAY was linearized by restriction digestion. The fragments were confirmed by agarose gel electrophoresis and these were ligated together with pIMAY and electroporated into *E. coli* DC10B. DC10B was used as plasmids propagated in this strain can be transformed directly into *S. aureus* strains (98). Colonies which grew on both chloramphenicol, indicating plasmid presence, and erythromycin, indicating insert presence, were tested by colony PCR for total insert presence. Primers used were present in the upstream and downstream regions of 1984. 24 colonies were tested and four showed bands at ~2800 bp showing insert presence (Figure 10).

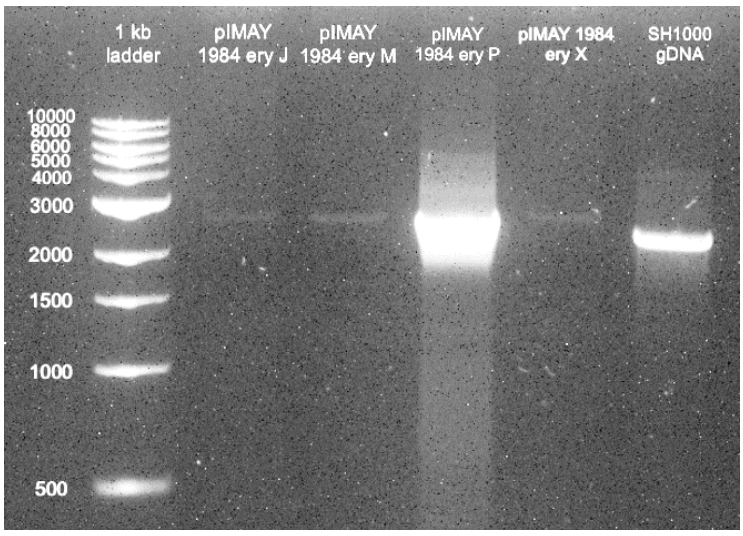


Figure 10. 1% agarose gel to check the presence of 1984 *erm* fragment from DC10B cells. This gel shows 4 colonies resistant to chloramphenicol and erythromycin. The numbers on the left indicate the size of each of the bands of the 1 kb in base pairs. Colonies were allocated letters when patched from the original transformation plate. Faint bands are seen for J, M and X and a strong band is seen for P at ~2800 bp indicating presence of 1984 flanking regions and *erm*. SH1000 gDNA was used as PCR positive control and a band is seen at ~2300 bp (far right) indicating presence of 1984 and the neighbouring regions.

Confirmation of the plasmids was carried out by digestion with EcoRI. All four plasmids appeared uncut indicating the inserts were located in the multiple cloning site (Figure 11). The plasmids were sequenced, and data showed the

upstream region of 1984 leading into *erm* and the 1984 downstream region for all four plasmids as expected.

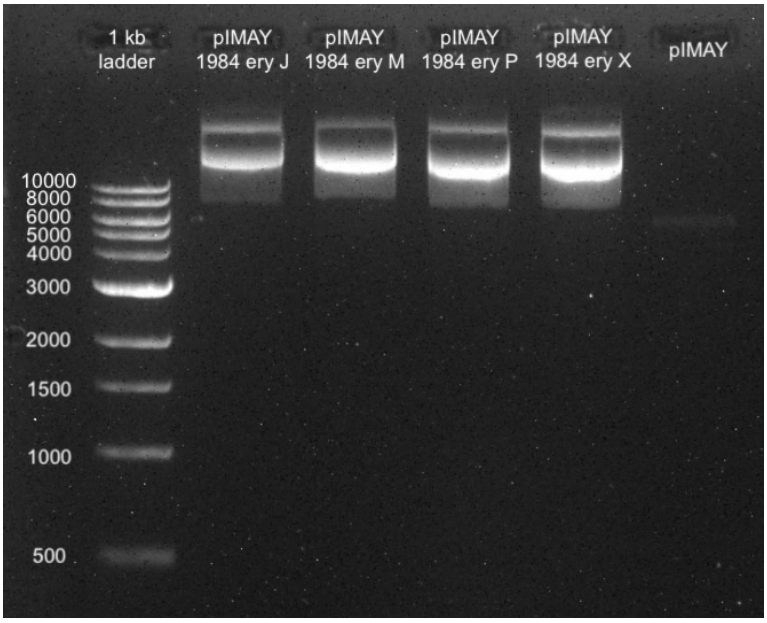


Figure 11. 1% agarose gel showing restriction digest of pIMAY 1984 *erm* plasmids and pIMAY empty vector control. All four plasmids have run as uncut plasmids indicating insertion into the multiple cloning site of EcoRI. pIMAY was digested as a positive control and has run as cut vector as 5743 bp (far right).

Electroporation of these plasmids was performed into *S. aureus* SH1000 and cells incubated at 28°C to enable plasmid replication (98). Colonies were seen on selective media however on propagation to fresh plates did not grow indicating these were false positive results. This would have to be repeated to move recombinant pIMAY into SH1000. The temperature sensitivity of pIMAY in SH1000 should be tested. The plasmid can lose this ability when cultured in *E. coli* and *E. coli* carrying pIMAY should have been grown at 37°C rather than 30°C to ensure this ability is maintained. The large size of the plasmid with inserts may also affect the electroporation as *S. aureus* does not transform with high efficiency.

The protocol would then be continued as described previously by Monk et al. to induce cross over of pIMAY into SH1000 and excision of plasmid DNA leaving *erm* in replacement of 1984 (98). This strain will be used in biofilm phenotype

experiments to determine the effect of knockout of 1984 on biofilm growth. Comparison of this to the *agr* mutant can help determine if 1984 is essential for *agr* function in biofilm growth.

3.4.3 *S. aureus* growth in artificial saliva media

Artificial saliva media was used to mimic the clinical site of biofilm growth in the mouth therefore growth of *S. aureus* strains in artificial saliva 1, 2 and TSB was compared. The final OD_{600} was lower in both artificial saliva media than in TSB for all strains except SH1000 lux where growth in both media was similar (Figure 12). SNAP tagged strains grew to a slightly lower final OD_{600} than non-SNAP tagged strains in all media. The SNAP tag presents on the outside of the cell and this appears to present a minor fitness cost.

Bioluminescence readings taken were normalised to the OD_{600}. The bioluminescence of Xen29 strains was higher than SH1000 strains and higher bioluminescence was seen for all strains in saliva media compared to TSB (Figure 12). Lux is expressed when the bacteria are metabolically active therefore the higher expression in both saliva media could indicate the bacteria are more metabolically active in these media than TSB. The final OD_{600} was higher in TSB than both artificial saliva media indicating this is a richer media however the cells appear to be less metabolically active from the bioluminescence level.

The bioluminescence of all strains is shown to decrease to negligible levels when the cells are in the stationary phase of growth. The strains possess a stable copy of a *Photorhabdus luminescens* modified complete lux operon. This expresses the luciferase enzyme and substrate therefore emits a constitutive bioluminescent signal when the bacteria are metabolically active (90). This would indicate that the bacteria are no longer metabolically active in the stationary phase. Kadurugamuwa et al. also saw a decrease in bioluminescence of Xen29 cells when in stationary phase. They noted that the bioluminescent signal was restored when the media was replaced indicating the decrease was due to oxygen limitations or accumulation of inhibitory molecules (88). Oxygen

is essential for bioluminescence therefore the decrease in signal could be due to oxygen depletion over time (99). This assay could be repeated under oxygen rich conditions or with replacement of media to determine if this is causing a reduction in bioluminescence.

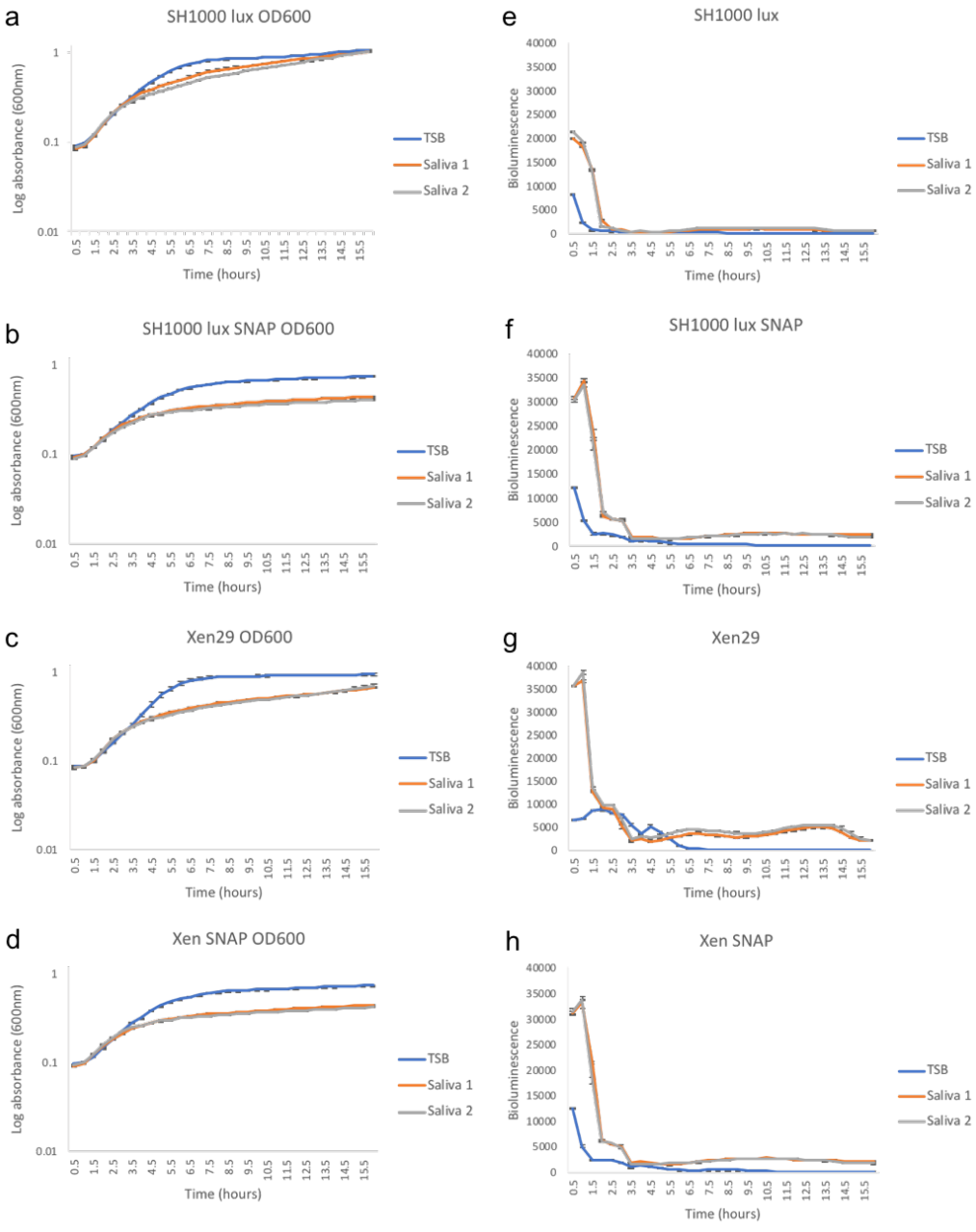


Figure 12. Growth curves of different *S. aureus* strains in TSB and artificial saliva media. a-d Log OD_{600} of each strain in each media. **e-h** bioluminescence of each strain in each media normalized to the OD_{600}.

3.4.4 *S. aureus* biofilm bead models

Comparison of *S. aureus* biofilm growth on 1.4 mm ceramic and smaller cytodex beads was performed in 10% TSB media. Lipophilic FM1-43 dye was used to visualise biofilms and determine the biomass using. FM1-43 is a lipid stain which fluoresces when incorporated into the outer leaflet of the cell membrane (100, 101). Biofilms were visualised via confocal microscopy and biofilm attachment sites were seen on ceramic beads which are smooth and uncharged (Figure 13). Cytodex beads are positively charged and contain pores which facilitates bacterial accumulation therefore it is hard to distinguish biofilm attachment sites (Figure 13).

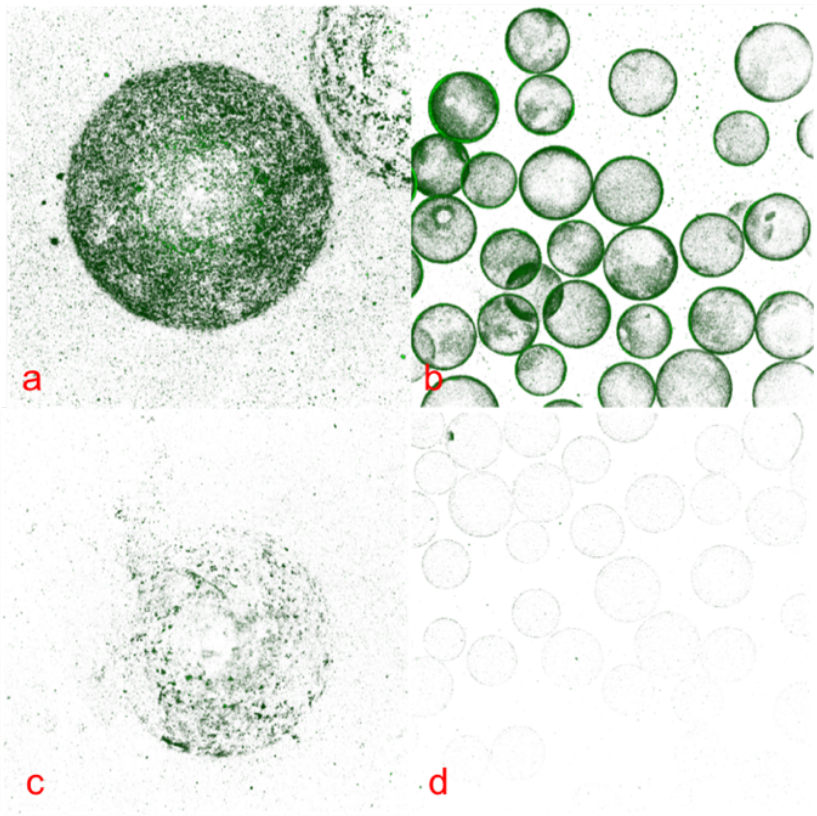


Figure 13. Maximum intensity projection images of biofilms grown in 10% TSB stained with FM1-43 imaged via confocal microscopy at 5x magnification. 6a: Xen Δ*agr* on a ceramic bead **6b:** Xen Δ*agr* on cytodex beads **6c:** Xen29 on a ceramic bead **6d:** Xen29 on cytodex beads. This shows biofilm attachment sites on ceramic beads and demonstrates the increase in biofilm biomass with the Xen Δ*agr* strain on both beads compared to wild type Xen29.

S. aureus Xen29 Δ*agr* biofilm growth was compared to wild type Xen29. The deletion of *agr* was expected to show an increase in biofilm biomass as downregulation of *agr* leads to production of thicker biofilms. Repression of *agr* induced RNAIII is essential for attachment and repression of AIP prevents cell detachment from the biofilm (66). This was supported by the results from this phenotypic assay as increased biofilm was seen with *agr* deletion strains than the wild type (Figure 13).

The bioluminescence of the biofilms on the beads should have been tested in order to determine if the cells emit a bioluminescent signal when the biofilm is established. Bioluminescence decreases over time as displayed in Figure 12. This could be due to low oxygen levels which are present in the biofilm and not all cells in the biofilm are proliferating or metabolically active. Previous *in vitro* models have shown that bioluminescence decreases when the cells reach stationary phase however the signal can be restored through replacement of the culture media every 12 hours (88). This should be considered in this model and the bioluminescence of the biofilm on the beads recorded. The variation in intensity of bioluminescence in the biofilm should represent the relative metabolic activity of cells at given locations in the biofilm and bioluminescent signal has been shown previously to correlate with viable cell numbers in a biofilm (88, 102).

3.4.5 Biofilms in artificial saliva media

From the growth curve data there was no noticeable difference in *S. aureus* growth for any of the strains in either of the saliva media and artificial saliva 1 was chosen for biofilm models. Biofilms were grown in an incubator, the micro vibrations and movement of the beads mimicking biofilm growth in the mouth. Biofilm was seen with all strains in artificial saliva media 1 on ceramic beads which were used as a tooth model. This proves *S. aureus* will readily form biofilm in the mouth. However, the artificial saliva media used was based on those used in the literature and antibacterial compounds present in the saliva were not taken into account (94-96). Components such as immunoglobulins, enzymes such as amylases, esterases and proteases, peptides, and non-

enzymatic proteins form a complex media which acts as an antimicrobial itself (103). Components of the immune system and enzymes aid in removal of bacteria before biofilm formation therefore should be taken into account when measuring oral biofilm growth to replicate conditions in the mouth more closely. The media could be developed to take into account components which would affect oral biofilm establishment and growth.

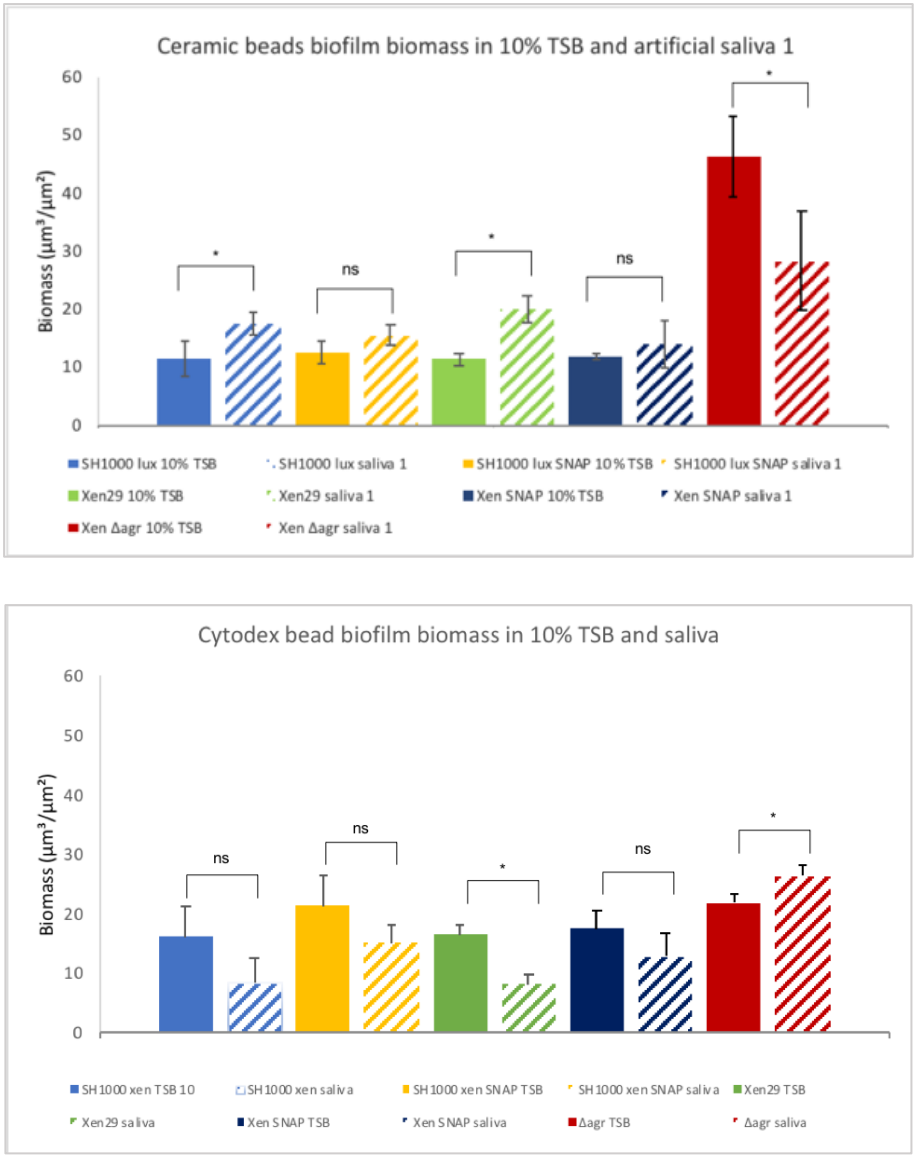


Figure 14. Biomass of biofilms on ceramic and cytodex beads in 10% TSB and artificial saliva media. Error bars display standard deviation. Students T-test analysis was performed and significant changes in biomass are marked with * ($P<0.05$), non-significant with ns. For ceramic beads the mean biomass from 3 beads is plotted for each strain for cytodex beads the mean biomass from 10 beads is plotted.

Biofilms were imaged via CLSM, Z stack images were taken of each biofilm and the biomass quantified using COMSTAT software (104). Three ceramic beads and ten cytodex beads were imaged per strain. COMSTAT analysis confirmed Xen29 Δ*agr* produced more biofilm biomass under all conditions than the wild type as described in the literature (Figure 14) (66). Similar biofilm growth is seen with non-SNAP and SNAP strains. This confirms that the SNAP tag which is linked to sortase and presents on the exterior of the cell is not affecting biofilm formation. Therefore, this strain can be used for biofilm models *in vivo* as there is no phenotypic difference from non-SNAP tagged strains.

On ceramic beads greater biofilm biomass was seen for non-mutant strains in artificial saliva 1 than 10% TSB however on cytodex beads more biomass was seen in 10% TSB than artificial saliva 1. Xen Δ*agr* showed the opposite trend in each media (Figure 14). The *agr* system is involved in control of biofilm growth and these results show that *agr* knockout affects biofilm growth in different media on different supports. This suggests that the *agr* system affects biofilm attachment and growth differently depending on the support and media.

This finding that *S. aureus* biofilm attachment differs depending on the support and media highlights the importance of developing *in vitro* models which will closely mimic the host environment. Biofilm formation differs depending on the environment therefore if is important to test attachment to materials used clinically *in vivo* such as catheters and clinically relevant media. This would inform about early biofilm attachment to these materials and could lead to the development of control strategies.

Variation in biofilm growth is seen therefore imaging multiple beads reduces bias by enabling quantification of biofilm from a predetermined number of beads per assay. Smaller ceramic beads would be a good model as these have no charge so would remove attachment bias and would enable high throughput visualisation of multiple biofilms. Cytodex beads are charged which will affect bacterial attachment therefore use of uncharged supports will

remove this interference. Additionally, more beads would need to be tested of each bead type in order to gain more significant results.

Furthermore, biofilms could be established on these beads with mixed populations of *S. aureus*. This will help determine how each strain attaches and if this is affected by the presence of other strains. Clinically biofilms are usually multispecies therefore using models with multiple strains will more closely replicate *in vivo* biofilm growth (86). Mixed populations of *agr* mutants, wild type and 1984 mutants could be used to determine how attachment changes. Identification of key elements in biofilm attachment will enable development of molecules which can target this. Newly established or establishing biofilms are much easier to treat than chronic biofilms therefore this would be a good antimicrobial target (67).

3.4.6 *S. aureus* biofilms stained with fluorescent probes

Fluorescent markers were used to monitor the spatial heterogeneity of the biofilm. 5-ethynyl-2'-deoxyuridine (EdU) was used to detect cell division. It is a thymidine analogue incorporated into DNA during DNA synthesis therefore is used to image replicating cells. It is detected via a 'click' reaction with Alexa Fluor 594 (92). EdU was first tested on planktonic Xen29 cells and imaged via CLSM (Figure 15). When stained with EdU the biomass of cells was lower than for unstained control indicating EdU may partially inhibit the cell cycle.

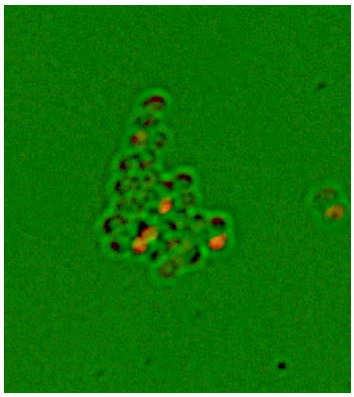


Figure 15. *S. aureus* Xen29 cells grown to mid log phase stained with EdU visualised with Alexa Fluor 594 seen coloured in red.

EdU was incubated with Xen29 biofilms overnight however when imaged no biofilm was seen indicating EdU inhibited biofilm growth. Therefore, EdU was added as an end point biofilm spike for one hour. Biofilms were then fixed with formal saline before addition of Alexa Fluor 594 for detection. Proliferating cells were seen stained in the outer layer of the biofilm (Figure 16 a-c). This indicated attached cells are not proliferating but outer cells are. The non-proliferating cells could be persistor cells which are dormant and can survive after antibiotic treatment (69). Investigating these cells and how they respond to antibiotic treatment could give insights into removal of metabolically inactive and dormant cells in the biofilm.

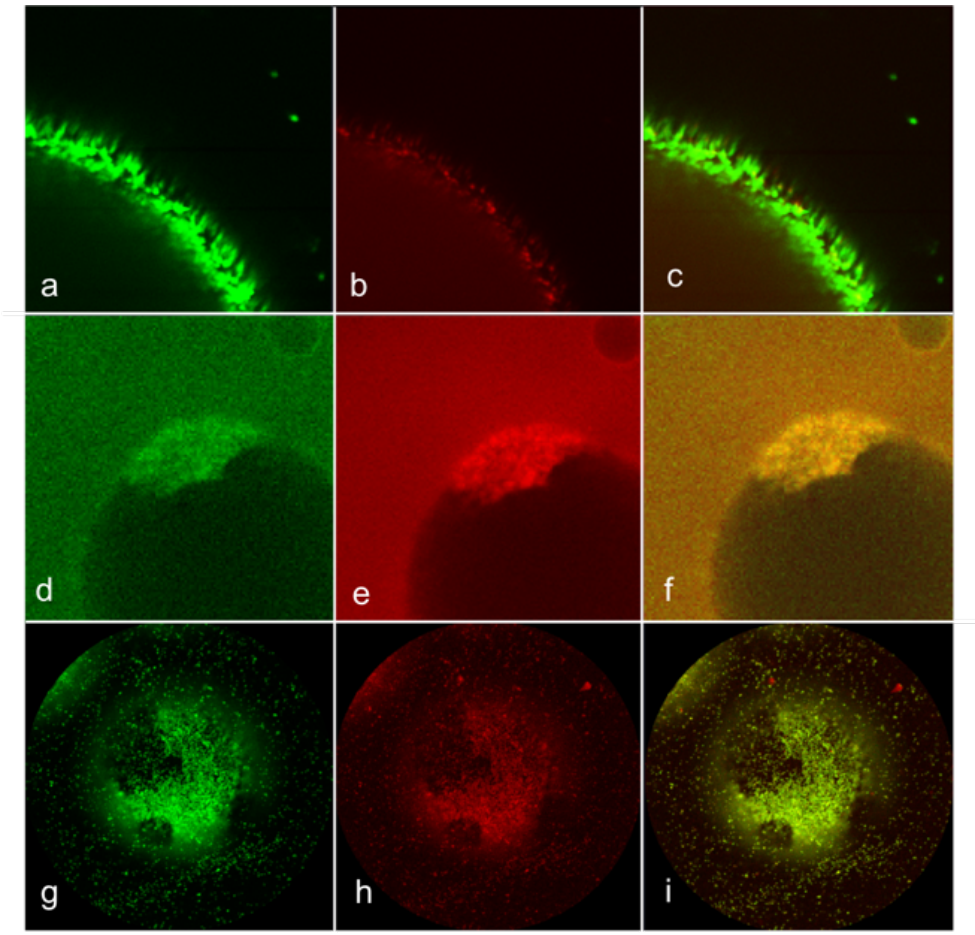


Figure 16. Xen29 biofilm grown on cytodex beads in 10% TSB. a) FM1-43 staining of biofilm on the edge of a cytodex bead **b)** EdU and Alexa Fluor 594 **c)** Colocalisation of FM1-43 and EdU. **d)** FM1-43 staining of cells in a pore of a cytodex bead **e)** OPP and Alexa Fluor 594 **f)** Colocalisation of FM1-43 and OPP. **g)** Calcein AM staining of the outside of a whole cytodex bead **h)** FM4-64 **i)** Colocalisation of calcein and FM4-64.

O-propargyl-puromycin (OPP) was used to stain protein synthesis, it is an analogue of puromycin, an aminonucleoside antibiotic which blocks protein synthesis by inducing premature termination of polypeptide chains. OPP forms covalent bonds with newly synthesised polypeptide chains and is detected with Alexa Fluor 594 (93). This also inhibited biofilm growth when incubated overnight so was added as an end point marker. Staining of cells undergoing protein synthesis in a pore on a cytodex bead was detected showing this dye was effective (Figure 16 d-f). OPP retains some protein synthesis inhibition activity which may be why biofilm growth was inhibited when incubated with OPP overnight (93).

Calcein-AM was used to detect metabolically active cells. It is membrane permeable and fluoresces when the acetomethoxy quencher is cleaved by intracellular esterases (105). Calcein-AM was added to biofilms with FM4-64 as lipid stain. Colocalization was seen with FM4-64 and calcein however not all cells in the biofilm were shown to be metabolically active (Figure 16 g-i).

These stains have all been tested preliminarily here and further validation of each of these would be necessary. Biofilms could be tested at different time points when more or less cells are expected to be active for example in exponential growth more cells should be stained showing cell division, protein synthesis or metabolism. Additionally, in order to confirm the stained cells are actually dividing, synthesising proteins or metabolically active, antibiotic could be added. For example, chloramphenicol inhibits protein synthesis therefore cells treated with chloramphenicol should not be stained with OPP. This should be used as a control to show there is no non-specific binding and to prove the fluorescing cells are undergoing protein synthesis. Additionally, the bioluminescent signal of cells in the biofilm should be compared to the calcein AM staining. Bioluminescence should also show the proportion of metabolically active cells therefore comparison of this to the proportion of cells stained with calcein will confirm the number of viable cells in the biofilm.

Once validated, these stains could be used simultaneously to determine if protein synthesis, metabolism and cell division occur in the same cells in the biofilm. This will display the heterogeneity of cells in the biofilm. Additional stains can be used such as a live/dead stain to determine the proportion of living cells. These stains can be used in the presence of antibiotics to determine the effect these have on cellular processes in cells in a biofilm.

Xen Δ*agr* should be used with these markers as these biofilms are thicker so it will be easier to see the spatial heterogeneity (76). Additionally, these markers have all been shown to stain eukaryotic cells therefore could be given to mice *in vivo* at the infection site to enable monitoring of the reaction of host cells to infection as well as biofilm cells (92, 93, 105). By testing these on cytodex bead models *in vitro* it is possible to see how this can be transferred *in vivo.*

3.4.7 *In vivo* virulence testing

Preliminary *in vivo* studies were performed with SH1000 lux and Xen29 in *Galleria mellonella* (wax worm) infection models. Wax worms are used for infection models as they have a short life span so can be used for high throughput studies to measure mortality. They can be used to test hypotheses which can later be translated into higher organisms (86). This assay was used to monitor the initial stages of acute infection and the role of innate immunity. Antimicrobials can also be injected to the worms to screen compounds before use in murine models (106). Additionally they can be used in biofilm models to screen for virulence genes, colonisation and biofilm forming factors (86).

An insufficient number of worms were tested in order to draw conclusions from these results (Figure 17), more replicates would need to be performed. This will then be performed with the SNAP tagged strains to determine if this affects virulence. Additionally, the virulence of the USA300 JE2 lux strain created in this study can be ascertained. USA300 strains display increased virulence due to expression of toxins such as Panton-Valentine leucocidin (PVL). However, similar virulence has been seen with USA300 and SH1000 in murine models as mice are resistance to PVL whereas humans are susceptible (87, 107).

Therefore, the virulence should be tested in wax worm infection models. The virulence of the *agr* and 1984 deletion strains could also be tested using this model. *agr* activation is involved in *S. aureus* virulence therefore deletion may decrease the virulence. Comparison of the virulence of *agr* and 1984 knockout strains would help determine the effect of this regulator in control of *S. aureus* virulence. Investigating the virulence of different strains and which genes are involved in controlling this such as *agr* is important in developing antimicrobials (80). A novel way of treating bacterial infections is to reduce the virulence of the infecting bacteria therefore identifying genes which are involved in control of this such as *agr* and 1984 could help in target identification.

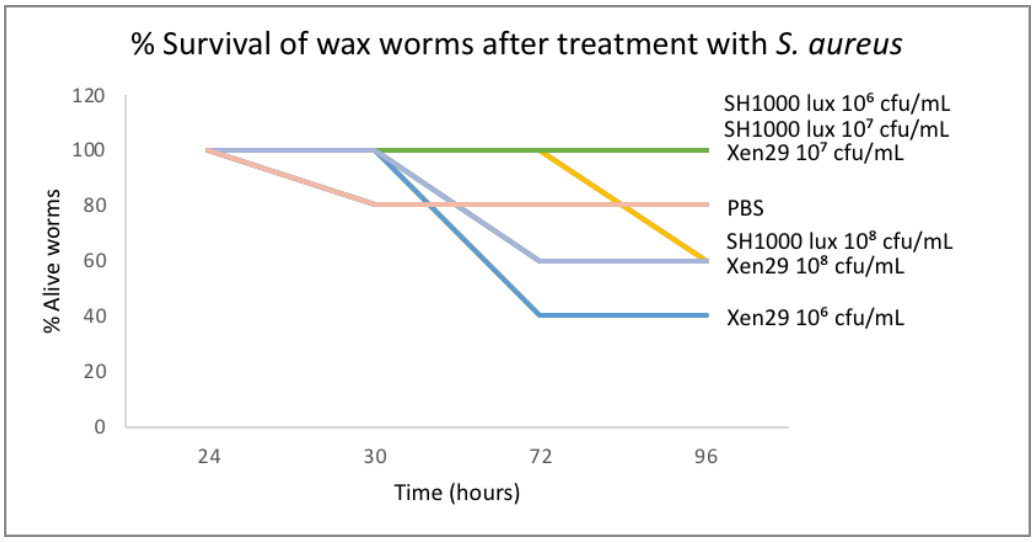


Figure 17. Survival of wax worms after treatment with *S. aureus.* 5 worms were tested per dilution.

Recently it has been noted that wax worms from the same source as those used here were pre-infected with staphylococci. These could be in competition with the *S. aureus* strains used in infection models and could interfere with the assays. Therefore, worms from an alternative source should also be tested.

Wax worms can also be injected with cytodex beads as a support for biofilm growth during virulence testing. The beads and biofilms can be recovered from the worm after infection. Analysis of these and comparison to the bacteria used in infection will help determine the state of the bacteria during the establishment of infection and biofilms. Biofilms on cytodex beads can by

analysed using confocal microscopy and the tools described here. This will enable biofilm monitoring *in vivo* and will determine how the innate immune response responds to biofilm establishment.

3.4.8 Conclusions

The use of beads as biofilm supports was shown to be successful and will reduce bias when imaging via CLSM. A defined number of beads can be imaged per experiment to enable non-biased screening. Analysis of the spatial organisation of cells in the biofilm using fluorescent markers can be performed and developed to enable improvement of strategies for tackling biofilms and discovery of new drug targets (108). The JE2 lux strain created and 1984 knockout strain will be tested with the tools used to evaluate the biofilm formation and their virulence.

4 Future perspectives

4.1 Antimicrobial resistance plasmids

In order to carry this project forward, further attempts must be made to transfer pNDM-HK *gfp* into a clinically relevant host to use as a plasmid donor as described previously. Once this is achieved the transmission of pNDM-HK into clinically relevant strains can be monitored using the flow cytometry-based assay to determine the proportion of bacterial cells the plasmid has transferred into and calculate the frequency of conjugation. Potential conjugation inhibitors can then be screened using this assay in a relatively high throughput manner to determine molecules which will reduce the spread of pNDM-HK clinically. Inhibitors can be applied and the difference in plasmid transmission quantified using flow cytometry to determine if a lower proportion of cells have acquired the plasmid than in the absence of the inhibitor. This will then be developed for use in multispecies environments. pNDM-HK *gfp* will be transferred to a donor strain expressing *mcherry* and transmission measured in multispecies settings to identify the strains the plasmid moves between in complex environments such as the GI tract.

Establishment of the assay to monitor pCT *gfp* and pKpQIL *gfp* transmission in multispecies environments will be completed. *mcherry* expressing bacteria carrying the plasmids will be used as donors in multispecies transmission experiments. When these are established, conjugation inhibitors identified in single species transmission screening can be tested. This will determine if the molecule's inhibitory activity is species specific of if the effect is seen in mixed species environments.

This assay can also be developed to monitor plasmid transmission in biofilms. Biofilms have been shown *in vitro* to facilitate the transfer of resistance genes and increased plasmid transfer of CTX-M-15 has been seen in *K. pneumoniae* biofilms compared to planktonic growth (86). This assay will determine if increased conjugation of these clinical plasmids is seen when cells are in single

or multispecies biofilms. Additionally, screening and development of inhibitors of conjugation in biofilms could be useful in preventing the spread of ARGs.

Once conjugation inhibitors have been identified using the flow cytometry screening method, research should focus on identifying the mechanism of action of the compounds. Identifying how compounds inhibit conjugation and their molecular targets will facilitate identification of other compounds which may target the same processes. Other compounds with similar structures could be tested using the same assay to determine if these also carry anti-conjugation activity. Previously FDA approved drugs should be screened using these assays. Use of drugs already in clinical use will mean that they are safe for use in humans therefore are more likely to have potential therapeutic use and could be given in combination with antibiotics. This would prevent the spread of ARGs in response to antibiotic stress.

Additionally, anti-conjugation compounds discovered which are not appropriate for use clinically should not be discounted. These could be used in other environments where conjugation and the spread of ARGs is seen such as in hospitals particularly on sinks, handrails and in wastewater pipes where bla_{KPC} and bla_{NDM} have both been isolated (109). This will help prevent the spread of antibiotic resistance plasmids in the hospital environment and help to remove the reservoir of ARGs. The transfer of plasmids should be monitored on different surfaces such as those found in hospitals. This will inform about how plasmid transfer will occur in the hospital environment and enable development of inhibitors. As well as this plasmid transmission in specific media can be monitored such as in waste water. This will enable assessment of transmission and inhibitor development for use in real world environments. Plasmid conjugation inhibitors could be used to prevent the spread of ARGs in the hospital and community environments to reduce the reservoir or ARGs and slow the spread of AMR.

4.2 Investigation of *S. aureus* biofilms

Investigation of *S. aureus* biofilms will enable improvement of strategies for tackling them and will help discovery of new drug targets. Further work associated with this project would involve completion of the SH1000 1984 knockout strain. Knockout of this novel regulator will enable further study to elucidate its role and determine if it is a potential therapeutic target. This knockout will also be induced in Xen29 and compared to wild type Xen29 and Xen Δ*agr* in phenotypic biofilm models. This will inform on the role of this novel regulator of the *agr* system in biofilm establishment and growth.

The *agr* and 1984 knockout strains will also be used in *Galleria mellonella* virulence models. The *agr* system is involved in control of *S. aureus* virulence therefore knockout of this system should reduce pathogenicity. Comparison of the virulence of the 1984 and *agr* knockouts will inform whether this regulator is involved in control of *S. aureus* virulence. If knockout of 1984 reduces pathogenicity of the bacteria in this model, this regulator could be a potential therapeutic target. This would reduce the disease-causing potential of the bacterium in infections and would make infections easier to control without using classic antibiotics.

These screens will help to determine the role of this regulator in *S. aureus* virulence and biofilm formation. Future work will involve further research into the role of this regulator in control of the *agr* system and determination if this is a potential target for control of *S. aureus* infections.

In vivo biofilms are not usually single species therefore mixed species biofilms will be investigated using the biofilm models tested here. Fluorescent markers can be used to tag individual species which will help to determine how these arrange in the biofilm. This will show the heterogeneity of multispecies biofilms and how the different species localise and interact (91). Biofilms with multiple *S. aureus* strains will be used in biofilm models such as Xen29 wild type, Xen Δ*agr*, and Xen Δ1984. This will determine if the presence of strains with different biofilm forming potential will affect attachment and establishment of

biofilms of other strains. Attachment of these to different surfaces under different conditions will be evaluated.

Further validation and analysis will be performed with the fluorescent markers for visualisation of cellular processes via confocal microscopy as described previously. These can be used to determine the effect of antibiotic treatment on biofilms. Antibiotics will have different effects on cells in the biofilm depending on their localisation and their activity. Using this imaging technique, it will be possible to evaluate how an antibiotic affects different cell processes and how far it penetrates into the biofilm. Additionally, the heterogeneity of biofilms after antibiotic treatment has ended can be determined. This will show if previously dormant or non-metabolically active cells reactivate after the antibiotic threat is removed. Using COMSTAT analysis software it will be possible to calculate the proportion of cells in the biofilm in each state before, during and after antibiotic treatment.

This study involved validating tools in the lab which can be used to look at the *in vivo* infection site. All of the markers used in this project have been shown to stain eukaryotic cells therefore they can be used *in vivo* after *in vitro* validation (92, 93, 105). Use of these *in vivo* in murine infections models will enable monitoring of host cells and how they react to biofilm infection. Certain host cell types can be tagged, for example macrophages, in order to monitor the infiltration of these immune cells into the infection site. Monitoring the spatial arrangement as well as the cellular activities of these immune cells will inform about how these react to biofilm growth. Biofilm cells can be monitored simultaneously to determine the effect of the immune response and antibiotic treatment on biofilms *in vivo*. Biofilms will be grown *in vivo* on bead supports such as the cytodex beads. These will be removed from the mouse with the surrounding tissue after infection and analysed via confocal microscopy. Clinical biofilm growth is difficult to replicate *in vitro* therefore it is important to analyse biofilm establishment, growth and response to antibiotic treatment and the immune response *in vivo.* This will further understanding of *S. aureus* biofilm establishment and response to antimicrobial and immune attack.

Therefore, this will enable improvement of strategies for tackling biofilms and lead to the discovery of new drug targets.

References

1. C. L. Ventola, The antibiotic resistance crisis: part 1: causes and threats. *P & T* 40, 277-283 (2015).
2. J. L. Martinez, F. Baquero, Emergence and spread of antibiotic resistance: setting a parameter space. *Ups J Med Sci* 119, 68-77 (2014).
3. S. Sengupta, M. K. Chattopadhyay, H. P. Grossart, The multifaceted roles of antibiotics and antibiotic resistance in nature. *Front Microbiol* 4, 47 (2013).
4. K. Gould, Antibiotics: from prehistory to the present day. *J Antimicrob Chemother* 71, 572-575 (2016).
5. R. I. Aminov, A brief history of the antibiotic era: lessons learned and challenges for the future. *Front Microbiol* 1, 134 (2010).
6. L. Katz, R. H. Baltz, Natural product discovery: past, present, and future. *J Ind Microbiol Biotechnol* 43, 155-176 (2016).
7. B. H. Normark, S. Normark, Evolution and spread of antibiotic resistance. *J Intern Med* 252, 91-106 (2002).
8. B. Spellberg, D. N. Gilbert, The future of antibiotics and resistance: a tribute to a career of leadership by John Bartlett. *Clin Infect Dis* 59 Suppl 2, S71-75 (2014).
9. J. M. Munita, C. A. Arias, Mechanisms of Antibiotic Resistance. *Microbiol Spectr* 4 (2016).
10. A. F. Read, R. J. Woods, Antibiotic resistance management. *Evol Med Public Health*. vol. 2014, pp. 147 (2014).
11. C. A. Michael, D. Dominey-Howes, M. Labbate, The antimicrobial resistance crisis: causes, consequences, and management. *Front Public Health* 2, 145 (2014).
12. N. K. Archer, M.J. Mazaitis, J.W. Costerton, J. G. Leid, M. E. Powers, M. E. Shirtliff, Staphylococcus aureus biofilms: properties, regulation, and roles in human disease. Virulence 2, 445-459 (2011).

13. R. M. Donlan, Role of biofilms in antimicrobial resistance. *Asaio j* 46, S47-52 (2000).
14. P. Nordmann, G. Cuzon, T. Naas, The real threat of Klebsiella pneumoniae carbapenemase-producing bacteria. *Lancet Infect Dis* 9, 228-236 (2009).
15. J. O'Neill, Tackling Drug -Resistant Infections Globally: Final Report and Recommendations the Review on Antimicrobial Resistance (2016).
16. K. Bush, P. Courvalin, G. Dantas, J. Davies, B. Eisenstein, P. Huovinen, G. A Jacoby, R. Kishony, B. N. Kreiswirth, E. Kutter, S. A. Lerner, S. Levy, K. Lewis, O. Lomovskaya, J. H. Miller, S. Mobashery, L. J. Piddock, S. Projan, C. M. Thomas, A. Tomasz, P. M Tulkens, T. R. Walsh, J. D. Watson, J. Witkowski, W. Witte, G. Wright, P. Yeh, H. I. Zgurskaya, Tackling antibiotic resistance. *Nat Rev Microbiol* 9, 894-896 (2011).
17. F. M. Aarestrup, V. F. Jensen, H. D. Emborg, E. Jacobsen, H. C. Wegener, Changes in the use of antimicrobials and the effects on productivity of swine farms in Denmark. *Am J Vet Res* 71, 726-733 (2010).
18. W. Wohlleben, Y. Mast, E. Stegmann, N. Ziemert, Antibiotic drug discovery. *Microb Biotechnol* 9, 541-548 (2016).
19. E. Cabezon, F. de la Cruz, I. Arechaga, Conjugation Inhibitors and Their Potential Use to Prevent Dissemination of Antibiotic Resistance Genes in Bacteria. *Front Microbiol* 8, 2329 (2017).
20. M. Getino, D. J. Sanabria-Rios, R. Fernandez-Lopez, J. Campos-Gomez, J. M. Sanchez-Lopez, A. Fernandez, N. M. Carballeira. F. de la Cruz, Synthetic Fatty Acids Prevent Plasmid-Mediated Horizontal Gene Transfer. *MBio* 6, e01032-01015 (2015).
21. F. Baquero, T. M. Coque, F. de la Cruz, Ecology and evolution as targets: the need for novel eco-evo drugs and strategies to fight antibiotic resistance. *Antimicrob Agents Chemother* 55, 3649-3660 (2011).
22. WHO, Global priority list of antibiotic-resistant bacteria to guide research, discovery, and development of new antibiotics (2017).
23. F. E. Graf, M. Palm, J. Warringer, A. Farewell, Inhibiting conjugation as a tool in the fight against antibiotic resistance. *Drug Dev Res* (2018).

24. P. M. Bennett, Plasmid encoded antibiotic resistance: acquisition and transfer of antibiotic resistance genes in bacteria. *Br J Pharmacol* 153 Suppl 1, S347-357 (2008).
25. M. N. Alekshun, S. B. Levy, Molecular mechanisms of antibacterial multidrug resistance. *Cell* 128, 1037-1050 (2007).
26. S. M. Soucy, J. Huang, J. P. Gogarten, Horizontal gene transfer: building the web of life. *Nat Rev Genet* 16, 472-482 (2015).
27. M. M. C. Buckner, M. L. Ciusa, L. J. V. Piddock, Strategies to combat antimicrobial resistance: anti-plasmid and plasmid curing. *FEMS Microbiol Rev* 42, 781-804 (2018).
28. R. P. Novick, Plasmid incompatibility. *Microbiol Rev* 51, 381-395 (1987).
29. M. Rozwandowicz, M. S. M. Brouwer, J. Fischer, J. A. Wagenaar, B. Gonzalez-Zorn, B. Guerra, D. J. Mevius, J. Hordijk, Plasmids carrying antimicrobial resistance genes in Enterobacteriaceae. *J Antimicrob Chemother* 73, 1121-1137 (2018).
30. M. Getino, F. de la Cruz, Natural and Artificial Strategies To Control the Conjugative Transmission of Plasmids. *Microbiol Spectr* 6 (2018).
31. P. L. Ho, W. U. Lo, M. K. Yeung, C. H. Lin, K. H. Chow, I. Ang, A. H. Tong, J. Y. Bao, S. Lok, J. Y. Lo, Complete sequencing of pNDM-HK encoding NDM-1 carbapenemase from a multidrug-resistant Escherichia coli strain isolated in Hong Kong. *PLoS One* 6, e17989 (2011).
32. J. D. Anderson, The effect of R-factor carriage on the survival of Escherichia coli in the human intestine. *J Med Microbiol* 7, 85-90 (1974).
33. A. J. Lopatkin H. R. Meredith, J. K. Srimani, C. Pfeiffer, R. Durrett, L. You, Persistence and reversal of plasmid-mediated antibiotic resistance. *Nat Commun* 8, 1689 (2017).
34. J. L. Cottell, M. A. Webber, L. J. Piddock, Persistence of transferable extended-spectrum-beta-lactamase resistance in the absence of antibiotic pressure. *Antimicrob Agents Chemother* 56, 4703-4706 (2012).
35. A. McNally, Y. Oren, D. Kelly, B. Pascoe, S. Dunn, T. Sreecharan, M. Vehkala, N. Valimaki, M. B. Prentice, A. Ashour, O. Avram, T. Pupko, U.

Dobrindt, I. Literak, S. Guenther, K. Schaufler, L. H. Wieler, Z. Zhiyong, S. K. Sheppard, J. O. McInerney, J. Corander, Combined Analysis of Variation in Core, Accessory and Regulatory Genome Regions Provides a Super-Resolution View into the Evolution of Bacterial Populations. *PLoS Genet* 12, e1006280 (2016).

36. E. R. Bevan, A. M. Jones, P. M. Hawkey, Global epidemiology of CTX-M beta-lactamases: temporal and geographical shifts in genotype. *J Antimicrob Chemother* 72, 2145-2155 (2017).
37. A. U. Khan, L. Maryam, R. Zarrilli, Structure, Genetics and Worldwide Spread of New Delhi Metallo-beta-lactamase (NDM): a threat to public health. *BMC Microbiol* 17, 101 (2017).
38. M. Doumith, J. Findlay, H. Hirani, K. L. Hopkins, D. M. Livermore, A. Dodgson, N. Woodford, Major role of pKpQIL-like plasmids in the early dissemination of KPC-type carbapenemases in the UK. *J Antimicrob Chemother* 72, 2241-2248 (2017).
39. J. Findlay, K. L. Hopkins, M. Doumith, D. Meunier, C. Wiuff, R. Hill, R. Pike, R. Loy, N. Mustafa, D. M. Livermore, N. Woodford, KPC enzymes in the UK: an analysis of the first 160 cases outside the North-West region. *J Antimicrob Chemother* 71, 1199-1206 (2016).
40. S. Navon-Venezia, K. Kondratyeva, A. Carattoli, Klebsiella pneumoniae: a major worldwide source and shuttle for antibiotic resistance. *FEMS Microbiol Rev* 41, 252-275 (2017).
41. A. Leavitt, I. Chmelnitsky, I. Ofek, Y. Carmeli, S. Navon-Venezia, Plasmid pKpQIL encoding KPC-3 and TEM-1 confers carbapenem resistance in an extremely drug-resistant epidemic Klebsiella pneumoniae strain. *J Antimicrob Chemother* 65, 243-248 (2010).
42. L. S. Tzouvelekis, A. Markogiannakis, M. Psichogiou, P. T. Tassios, G. L. Daikos, Carbapenemases in Klebsiella pneumoniae and other Enterobacteriaceae: an evolving crisis of global dimensions. *Clin Microbiol Rev* 25, 682-707 (2012).
43. J. L. Cottell, M. A. Webber, N. G. Coldham, D. L. Taylor, A. M. Cerdeno-Tarraga, H. Hauser, N. R. Thomson, M. J. Woodward, L. J. Piddock,

Complete sequence and molecular epidemiology of IncK epidemic plasmid encoding blaCTX-M-14. *Emerg Infect Dis* 17, 645-652 (2011).

44. H. Dhanji, P. Khan, J. L. Cottell, L. J. Piddock, J. Zhang, D. M. Livermore, N. Woodford, Dissemination of pCT-like IncK plasmids harboring CTX-M-14 extended-spectrum beta-lactamase among clinical Escherichia coli isolates in the United Kingdom. *Antimicrob Agents Chemother* 56, 3376-3377 (2012).
45. A. Carattoli, Resistance plasmid families in Enterobacteriaceae. *Antimicrob Agents Chemother* 53, 2227-2238 (2009).
46. A. Carattoli, A. Bertini, L. Villa, V. Falbo, K. L. Hopkins, E. J. Threlfall, Identification of plasmids by PCR-based replicon typing. *J Microbiol Methods* 63, 219-228 (2005).
47. J. M. Andrews, Determination of minimum inhibitory concentrations. *J Antimicrob Chemother* 48 Suppl 1, 5-16 (2001).
48. EMBL-EBI, , Clustal Omega, [online], https://www.ebi.ac.uk/Tools/msa/clustalo/, (2019).
49. A. Sugino, C. L. Peebles, K. N. Kreuzer, N. R. Cozzarelli, Mechanism of action of nalidixic acid: purification of Escherichia coli nalA gene product and its relationship to DNA gyrase and a novel nicking-closing enzyme. *Proc Natl Acad Sci U S A* 74, 4767-4771 (1977).
50. W. Wehrli, Rifampin: mechanisms of action and resistance. *Rev Infect Dis* 5 Suppl 3, S407-411 (1983).
51. A. Cullik, Y. Pfeifer, R. Prager, H. von Baum, W. Witte, A novel IS26 structure surrounds blaCTX-M genes in different plasmids from German clinical Escherichia coli isolates. *J Med Microbiol* 59, 580-587 (2010).
52. A. Kottara, J. P. J. Hall, E. Harrison, M. A. Brockhurst, Variable plasmid fitness effects and mobile genetic element dynamics across Pseudomonas species. *FEMS Microbiol Ecol* 94 (2018).
53. C. T. Bergstrom, M. Lipsitch, B. R. Levin, Natural selection, infectious transfer and the existence conditions for bacterial plasmids. *Genetics* 155, 1505-1519 (2000).

54. L. Roer, F. M. Aarestrup, H. Hasman, The EcoKI type I restriction-modification system in Escherichia coli affects but is not an absolute barrier for conjugation. *J Bacteriol* 197, 337-342 (2015).
55. D. C. Hooper, Mechanisms of action and resistance of older and newer fluoroquinolones. *Clin Infect Dis* 31 Suppl 2, S24-28 (2000).
56. Y. Saenz, M. Zarazaga, L. Brinas, F. Ruiz-Larrea, C. Torres, Mutations in gyrA and parC genes in nalidixic acid-resistant Escherichia coli strains from food products, humans and animals. *J Antimicrob Chemother* 51, 1001-1005 (2003).
57. A. M. George, R. M. Hall, H. W. Stokes, Multidrug resistance in Klebsiella pneumoniae: a novel gene, ramA, confers a multidrug resistance phenotype in Escherichia coli. *Microbiology* 141 (Pt 8), 1909-1920 (1995).
58. F. J. Chen, T. L. Lauderdale, M. Ho, H. J. Lo, The roles of mutations in gyrA, parC, and ompK35 in fluoroquinolone resistance in Klebsiella pneumoniae. *Microb Drug Resist* 9, 265-271 (2003).
59. J. E. Barrick, M. R. Kauth, C. C. Strelioff, R. E. Lenski, Escherichia coli rpoB mutants have increased evolvability in proportion to their fitness defects. *Mol Biol Evol* 27, 1338-1347 (2010).
60. M. Xu, Y. N. Zhou, B. P. Goldstein, D. J. Jin, Cross-resistance of Escherichia coli RNA polymerases conferring rifampin resistance to different antibiotics. *J Bacteriol* 187, 2783-2792 (2005).
61. K. A. Datsenko, B. L. Wanner, One-step inactivation of chromosomal genes in Escherichia coli K-12 using PCR products. *Proc Natl Acad Sci U S A* 97, 6640-6645 (2000).
62. M. Bhattacharya, D. J. Wozniak, P. Stoodley, L. Hall-Stoodley, Prevention and treatment of Staphylococcus aureus biofilms. *Expert Rev Anti Infect Ther* 13, 1499-1516 (2015).
63. S. Y. Tong, J. S. Davis, E. Eichenberger, T. L. Holland, V. G. Fowler, Jr., Staphylococcus aureus infections: epidemiology, pathophysiology, clinical manifestations, and management. *Clin Microbiol Rev* 28, 603-661 (2015).

64. S. G. Woo, S. Y. Lee, S. M. Lee, K. H. Kim, E. J. Ha, Y. B. Eom, Activity of novel inhibitors of Staphylococcus aureus biofilms. *Folia Microbiol (Praha)* 62, 157-167 (2017).

65. J. L. Lister, A. R. Horswill, Staphylococcus aureus biofilms: recent developments in biofilm dispersal. *Front Cell Infect Microbiol* 4, 178 (2014).

66. B. R. Boles, A. R. Horswill, Agr-mediated dispersal of Staphylococcus aureus biofilms. *PLoS Pathog* 4, e1000052 (2008).

67. O. Ciofu, T. Tolker-Nielsen, Tolerance and Resistance of Pseudomonas aeruginosa Biofilms to Antimicrobial Agents-How P. aeruginosa Can Escape Antibiotics. *Front Microbiol* 10, 913 (2019).

68. P. Speziale, J. A. Geoghegan, Biofilm formation by staphylococci and streptococci: structural, functional, and regulatory aspects and implications for pathogenesis. *Front Cell Infect Microbiol* 5, 31 (2015).

69. K. Lewis, Persister cells and the riddle of biofilm survival. *Biochemistry (Mosc)* 70, 267-274 (2005).

70. M. Otto, Staphylococcal biofilms. *Curr Top Microbiol Immunol* 322, 207-228 (2008).

71. R. M. Donlan, Biofilms: microbial life on surfaces. *Emerg Infect Dis* 8, 881-890 (2002).

72. K. E. Traber, E. Lee, S. Benson, R. Corrigan, M. Cantera, B. Shopsin, R. P. Novick, agr function in clinical Staphylococcus aureus isolates. *Microbiology* 154, 2265-2274 (2008).

73. J. S. Wright, 3rd, R. Jin, R. P. Novick, Transient interference with staphylococcal quorum sensing blocks abscess formation. *Proc Natl Acad Sci U S A* 102, 1691-1696 (2005).

74. K. F. Kong, C. Vuong, M. Otto, Staphylococcus quorum sensing in biofilm formation and infection. *Int J Med Microbiol* 296, 133-139 (2006).

75. J. M. Yarwood, D. J. Bartels, E. M. Volper, E. P. Greenberg, Quorum sensing in Staphylococcus aureus biofilms. *J Bacteriol* 186, 1838-1850 (2004).

76. C. Vuong, H. L. Saenz, F. Gotz, M. Otto, Impact of the agr quorum-sensing system on adherence to polystyrene in Staphylococcus aureus. *J Infect Dis* 182, 1688-1693 (2000).

77. R. P. Novick, E. Geisinger, Quorum sensing in staphylococci. *Annu Rev Genet* 42, 541-564 (2008).

78. J. M. Yarwood, P. M. Schlievert, Quorum sensing in Staphylococcus infections. *J Clin Invest* 112, 1620-1625 (2003).

79. B. Gray, P. Hall, H. Gresham, Targeting agr- and agr-Like quorum sensing systems for development of common therapeutics to treat multiple gram-positive bacterial infections. *Sensors (Basel)* 13, 5130-5166 (2013).

80. L. Tan, S. R. Li, B. Jiang, X. M. Hu, S. Li, Therapeutic Targeting of the Staphylococcus aureus Accessory Gene Regulator (agr) System. *Front Microbiol* 9, 55 (2018).

81. G. Brackman, P. Cos, L. Maes, H. J. Nelis, T. Coenye, Quorum sensing inhibitors increase the susceptibility of bacterial biofilms to antibiotics in vitro and in vivo. *Antimicrob Agents Chemother* 55, 2655-2661 (2011).

82. S. Marroquin, B. Gimza, B. Tomlinson, M. Stein, A. Frey, R. A. Keogh, R. Zapf, D. A. Todd, N. B. Cech, R. K. Carroll, L. N. Shaw, MroQ Is a Novel Abi-Domain Protein That Influences Virulence Gene Expression in Staphylococcus aureus via Modulation of Agr Activity. *Infect Immun* 87 (2019).

83. Y. Ohara-Nemoto, H. Haraga, S. Kimura, T. K. Nemoto, Occurrence of staphylococci in the oral cavities of healthy adults and nasal oral trafficking of the bacteria. *J Med Microbiol* 57, 95-99 (2008).

84. H. Wang, D. Ren, Controlling Streptococcus mutans and Staphylococcus aureus biofilms with direct current and chlorhexidine. *AMB Express* 7, 204 (2017).

85. A. J. Smith, M. S. Jackson, J. Bagg, The ecology of Staphylococcus species in the oral cavity. *J Med Microbiol* 50, 940-946 (2001).

86. D. Lebeaux, A. Chauhan, O. Rendueles, C. Beloin, From in vitro to in vivo Models of Bacterial Biofilm-Related Infections. *Pathogens* 2, 288-356 (2013).

87. J. S. Cho, J. Zussman, N. P. Donegan, R. I. Ramos, N. C. Garcia, D. Z. Uslan, Y. Iwakura, S. I. Simon, A. L. Cheung, R. L. Modlin, J. Kim, L. S. Miller, Noninvasive in vivo imaging to evaluate immune responses and antimicrobial therapy against Staphylococcus aureus and USA300 MRSA skin infections. *J Invest Dermatol* 131, 907-915 (2011).

88. J. L. Kadurugamuwa, L. Sin, E. Albert, J. Yu, K. Francis, M. DeBoer, M. Rubin, C. Bellinger-Kawahara, T. R. Parr Jr., P. R. Contag, Direct continuous method for monitoring biofilm infection in a mouse model. *Infect Immun* 71, 882-890 (2003).

89. K. P. Francis, D. Joh, C. Bellinger-Kawahara, M. J. Hawkinson, T. F. Purchio, P. R. Contag, Monitoring bioluminescent Staphylococcus aureus infections in living mice using a novel luxABCDE construct. *Infect Immun* 68, 3594-3600 (2000).

90. Y. Q. Xiong, J. Willard, J. L. Kadurugamuwa, J. Yu, K. P. Francis, A. S. Bayer, Real-time in vivo bioluminescent imaging for evaluating the efficacy of antibiotics in a rat Staphylococcus aureus endocarditis model. *Antimicrob Agents Chemother* 49, 380-387 (2005).

91. M. J. Franklin, C. Chang, T. Akiyama, B. Bothner, New Technologies for Studying Biofilms. *Microbiol Spectr* 3 (2015).

92. A. Salic, T. J. Mitchison, A chemical method for fast and sensitive detection of DNA synthesis in vivo. *Proc Natl Acad Sci U S A* 105, 2415-2420 (2008).

93. J. Liu, Y. Xu, D. Stoleru, A. Salic, Imaging protein synthesis in cells and tissues with an alkyne analog of puromycin. *Proc Natl Acad Sci U S A* 109, 413-418 (2012).

94. L. Sherry, G. Lappin, L. E. O'Donnell, E. Millhouse, O. R. Millington, D. J. Bradshaw, A. S. Axe, C. Williams, C. J. Nile, G. Ramage, Viable Compositional Analysis of an Eleven Species Oral Polymicrobial Biofilm. *Front Microbiol* 7, 912 (2016).

95. E. Millhouse, A. Jose, L, Sherry, D. F. Lappin, N. Patel, A. M. Middleton, J. Pratten, S. Culshaw, G. Ramage, Development of an in vitro periodontal biofilm model for assessing antimicrobial and host modulatory effects of bioactive molecules. *BMC Oral Health* 14, 80 (2014).

96. J. Pratten, A. W. Smith, M. Wilson, Response of single species biofilms and microcosm dental plaques to pulsing with chlorhexidine. *J Antimicrob Chemother* 42, 453-459 (1998).

97. E. Amaral, S. Guatimosim, C. Guatimosim, Using the fluorescent styryl dye FM1-43 to visualize synaptic vesicles exocytosis and endocytosis in motor nerve terminals. *Methods Mol Biol* 689, 137-148 (2011).

98. D. Bratosin, L. Mitrofan, C. Palii, J. Estaquier, J. Montreuil, Novel fluorescence assay using calcein-AM for the determination of human erythrocyte viability and aging. *Cytometry A* 66, 78-84 (2005).

99. T. L. Harris, R. J. Worthington, C. Melander, Potent small-molecule suppression of oxacillin resistance in methicillin-resistant Staphylococcus aureus. *Angew Chem Int Ed Engl* 51, 11254-11257 (2012).

100. I. R. Monk, I. M. Shah, M. Xu, M. W. Tan, T. J. Foster, Transforming the untransformable: application of direct transformation to manipulate genetically Staphylococcus aureus and Staphylococcus epidermidis. *MBio* 3 (2012).

101. C. Gregor, K. C. Gwosch, S. J. Sahl, S. W. Hell, Strongly enhanced bacterial bioluminescence with the ilux operon for single-cell imaging. *Proc Natl Acad Sci U S A* 115, 962-967 (2018).

102. D. Schneider, E. Fuhrmann, I. Scholz, W. R. Hess, P. L. Graumann, Fluorescence staining of live cyanobacterial cells suggest non-stringent chromosome segregation and absence of a connection between cytoplasmic and thylakoid membranes. *BMC Cell Biol* 8, 39 (2007).

103. J. L. Kadurugamuwa, L. V. Sin, J. Yu, K. P. Francis, R. Kimura, T. Purchio, P. R. Contag, Rapid direct method for monitoring antibiotics in a mouse

model of bacterial biofilm infection. *Antimicrob Agents Chemother* 47, 3130-3137 (2003).

104. G. H. Carpenter, The secretion, components, and properties of saliva. *Annu Rev Food Sci Technol* 4, 267-276 (2013).

105. A. Heydorn, A. T. Neilsen, M. Hentzer, C. Stenberg, M. Givskov, B. K. Ersboll, S. Molin, Quantification of biofilm structures by the novel computer program COMSTAT. *Microbiology* 146 (Pt 10), 2395-2407 (2000).

106. C. J. Tsai, J. M. Loh, T. Proft, Galleria mellonella infection models for the study of bacterial diseases and for antimicrobial drug testing. *Virulence* 7, 214-229 (2016).

107. B. A. Diep, L. Chan, P. Tattevin, O. Kajikawa, T. R. Martin, L. Basuino, T. T. Mai, H. Marbach, K. R. Braughton, A. R. Whitney, D. J. Gardner, X. Fan, C. W. Tseng, G. Y. Liu, C. Badiou, J. Etienne, G. Lina, M, A, Matthay, F. R. DeLeo, H. F. Chambers, Polymorphonuclear leukocytes mediate Staphylococcus aureus Panton-Valentine leukocidin-induced lung inflammation and injury. *Proc Natl Acad Sci U S A* 107, 5587-5592 (2010).

108. M. Guggenheim, S. Shapiro, R. Gmur, B. Guggenheim, Spatial arrangements and associative behavior of species in an in vitro oral biofilm model. *Appl Environ Microbiol* 67, 1343-1350 (2001).

109. R. A. Weingarten, R. C. Johnson, S. Conlan, A. M. Ramsburg, J. P. Dekker, A. F. Lau, P. Khil, R. T. Odom, C. Deming, M. Park, P. J. Thomas, D. K. Henderson, T. N. Palmore, J. A. Segre, K. M. Frank, Genomic Analysis of Hospital Plumbing Reveals Diverse Reservoir of Bacterial Plasmids Conferring Carbapenem Resistance. *MBio* 9 (2018).